Cerebral Cortex February 2007;17:475-491
doi:10.1093/cercor/bhj164
Advance Access publication March 31, 2006

The Ferret Auditory Cortex: Descending Projections to the Inferior Colliculus

Victoria M. Bajo, Fernando R. Nodal, Jennifer K. Bizley, David R. Moore[1] and Andrew J. King

Department of Physiology, Anatomy and Genetics, Sherrington Building, University of Oxford, Parks Road, Oxford OX1 3PT, UK
[1]Current address: Medical Research Council Institute of Hearing Research, University Park, Nottingham NG7 1BD, UK

Descending corticofugal projections are thought to play a critical role in shaping the responses of subcortical neurons. Here, we examine the origins and targets of ferret auditory corticocollicular projections. We show that the ectosylvian gyrus (EG), where the auditory cortex is located, can be subdivided into middle, anterior, and posterior regions according to the pattern of cytochrome oxidase staining and immunoreactivity for the neurofilament antibody SMI_{32}. Injection of retrograde tracers in the inferior colliculus (IC) labeled large layer V pyramidal cells throughout the EG and adjacent sulci. Each region of the EG has a different pattern of descending projections. Neurons in the primary auditory fields in the middle EG project to the lateral nucleus (LN) of the ipsilateral IC and bilaterally to the dorsal cortex and dorsal part of the central nucleus (CN). The projection to these dorsomedial regions of the IC is predominantly ipsilateral and topographically organized. The secondary cortical fields in the posterior EG target the same midbrain areas but exclude the CN of the IC. A smaller projection to the ipsilateral LN also arises from the anterior EG, which is the only region of auditory cortex to target tegmental areas surrounding the IC, including the superior colliculus, periaqueductal gray, intercollicular tegmentum, and cuneiform nucleus. This pattern of corticocollicular connectivity is consistent with regional differences in physiological properties and provides another basis for subdividing ferret auditory cortex into functionally distinct areas.

Keywords: anterograde labeling, ectosylvian gyrus, hearing, layer V pyramidal cells, midbrain, retrograde labeling

Introduction

The sensory areas of the neocortex can, via their extensive descending projections to the thalamus, midbrain, and other nuclei, have a profound effect on subcortical signal processing. Although the role of these corticofugal pathways is far from understood, it is clear from studies of different sensory modalities that cortical feedback can dynamically adjust the receptive fields and filtering properties of subcortical neurons (for recent reviews, see Suga and others 2002; Alitto and Usrey 2003; Winer 2005). This in turn will influence the information that is sent to the cortex via ascending pathways. Thus, rather than being at the top of a strict hierarchy, the cortex appears to make a significant contribution to processing at lower levels of the brain.

Although corticothalamic projections provide the largest descending pathways, there has recently been a lot of interest in the possible role played by axons from the cortex to the midbrain in facilitating the localization of multisensory signals (Stein 2005) and in mediating learning-induced plasticity within the brain (Suga and others 2002). Evidence for the latter possibility is provided by the finding that focal electrical stimulation of the auditory cortex can induce shifts in the frequency selectivity of neurons in the inferior colliculus (IC) (Yan and Suga 1998; Zhou and Jen 2000; Yan and others 2005), in their thresholds and dynamic ranges (Yan and Ehret 2002), and in their spatial (Jen and others 1998) and temporal (Ma and Suga 2001) response properties. It has also been proposed that the corticocollicular pathway is responsible for the IC plasticity that results from repetitive acoustic stimulation or auditory fear conditioning (Suga and others 2002). Although the behavioral significance of these modifications in IC response properties is largely unknown, a recent study from our own laboratory has shown that selective elimination of corticocollicular axons impairs the ability of adult ferrets to adapt their localization responses to abnormal spatial cues (Bajo and others 2006).

Learning-induced plasticity is a well-known property of the auditory cortex (Buonomano and Merzenich 1998). These findings therefore raise the possibility that descending cortical influences might enable similar experience-based changes to take place in the responses of midbrain neurons, suggesting that functions attributed to sensory areas of the cortex should actually be viewed as properties of cortical–midbrain circuits. Interpretation of the physiological changes reported in midbrain neurons following either focal stimulation or inactivation of particular regions of cortex requires a detailed understanding of the origins and targets of the corticocollicular projections. Moreover, characterization of regional differences in corticofugal connectivity is likely to provide valuable insights into the functional organization of different areas of the auditory cortex.

The anatomical organization of the auditory corticocollicular projections has been described in several mammalian species, including cats (Kelly and Wong 1981; Wong and Kelly 1981; Winer and others 1998; Winer and Prieto 2001; Winer 2005), rats (Saldaña and others 1996), bats (Marsh and others 2002), and gerbils (Bajo and Moore 2005). In this study, we set out to identify the pattern of descending projections to the IC in the ferret because this species has recently provided clear behavioral (King and Parsons 1999; Kacelnik and others 2006) and physiological (Fritz and others 2003, 2005) evidence for learning-induced plasticity in the mature auditory system.

Ferret auditory cortex is located in the ectosylvian gyrus (EG) of the temporal lobe and comprises 3 distinct areas in the middle, anterior, and posterior parts of the gyrus (MEG, AEG, and PEG, respectively), which have been distinguished on the basis of the distribution of sound-evoked 2-deoxyglucose activity (Wallace and others 1997). PEG has been subdivided into 2 areas according to the pattern of corticocortical connectivity and changes in the appearance of layer V (Pallas

and Sur 1993). Electrophysiological studies have mostly been restricted to the MEG and have identified 2 tonotopically organized primary fields, the primary auditory field (A1) (Kelly and others 1986; Phillips and others 1988) and the anterior auditory field (AAF) (Kowalski and others 1995). More recent intrinsic optical imaging (Nelken and others 2004) and electrophysiological recording studies (Bizley and others 2005) have confirmed this and identified a further 4 acoustically responsive regions, 2 located in the PEG and another 2 in the AEG.

By placing tracer injections into different regions of the IC and auditory cortex, we investigated the origin, distribution, and topography of the corticocollicular projection. A further aim of the study was to use this information to provide a better understanding of the different auditory areas in the ferret cortex. Preliminary results have been published in abstract form (Bajo and Moore 2002; Bizley and others 2003).

Materials and Methods

All experiments were approved by the local ethical review committee at the University of Oxford and licensed by the UK Home Office. Twenty-one healthy adult ferrets (*Mustela putorius furo*) bred and raised in our laboratory were used in this study. Neural tracers were injected in the IC in 12 cases and in different parts of the auditory cortex in 8 cases (Table 1 and Fig. 3). The remaining animal was used for Golgi staining.

The tracers used were 10% dextran tetramethylrhodamine (lysine fixable, 3000 and 10 000 MW, Fluororuby [FR]; Molecular Probes Inc., Eugene, OR), 10% biotinylated dextran amine (dextran biotin fixable) (BDA, 10 000 MW; Molecular Probes), 4% Fluorogold (FG; Fluorochrome Inc., Englewood, CO), and fluorescent latex microspheres (red and green retrobeads; Lumafluor Corp., Naples, FL) (Table 1).

After sedation with Domitor (0.1 mg/kg body weight intramuscularly [i.m.] of medetomidine hydrochloride; Pfizer Ltd, Kent, UK), anesthesia was induced with Saffan (2 ml/kg body weight i.m. of alfaxalone/alfadolone acetate; Schering-Plough Animal Health, Welwyn Garden City, UK) and maintained with an intravenous infusion of a mixture of Domitor (0.022 mg/kg/h) and Ketaset (5 mg/kg/h; ketamine hydrochloride; Fort Dodge Animal Health, Southampton, UK) in saline solution. Dexadreson (0.5 mg/kg/h of dexamethasone; Intervet UK Ltd, Milton Keynes, UK) and Atrocare (0.006 mg/kg/h of atropine sulfate; Animalcare Ltd, York, UK) were added to the infusate to avoid cerebral edema and minimize pulmonary secretions, respectively. Electrocardiogram was monitored, and body temperature was maintained at ~38 °C throughout the experimental procedure. Details of the number of injections made, the tracers used, and the injection site (IS) locations and sizes are provided in Table 1 and Figure 3. All animals received perioperative analgesia with Vetergesic (0.15 ml of buprenorphine hydrochloride, i.m.; Alstoe Animal Health, Melton Mowbray, UK).

Tracer Injections in the IC

The animal was mounted in a stereotaxic frame, a midline incision made in the scalp, and the left temporal muscle retracted to expose the skull at the level of the tentorium. After Marcain (bupivacaine hydrochloride, Astra Pharmaceuticals Ltd, Kings Langley, UK) infusion in the surgical wound, the left occipital cortex was exposed by a craniotomy. The dura mater was removed, and the most posterior corner of the occipital cortex carefully aspirated until the IC was visible. Tracers were injected through a glass micropipette with a 15- to 30-μm tip diameter at different lateromedial and dorsoventral IC locations. Every tracer injection was made in the left IC. BDA and FG were always injected by iontophoresis over a period of 15 min using a positive current of 5 μA with a duty cycle of 7 s. FR was also injected by iontophoresis using the same parameters, except for one case (F0061) where several pressure injections were made at different dorsoventral locations in 3 lateromedial penetrations in the IC. Retrobeads were always injected by pressure with a microinjector (Nanoject II; Drummond Scientific Company, Broomall, PA). Undiluted retrobeads were injected, whereas the other tracers used were diluted in 0.9% saline. The surface of the IC and surgical aspiration wound were covered by small pieces of Surgicel (Johnson & Johnson Ltd, Slough, UK), after which the piece of cranium was put back in place, and the temporal muscle and skin were sutured.

Table 1
List of animals and tracer injections used in this study

Animal number	Tracer used	Plane	Location of IS	Size of the IS (mm^3) center (halo)
F9969	FR	Coronal	Dorsomedial IC	0.03 (0.86)
	BDA		LN	0.06 (0.61)
F9959	BDA	Coronal	PAG	0.03 (0.08)
F0014	BDA	Coronal	Dorsomedial IC	0.04 (0.75)
F0061	FR	Horizontal	Large IC	—
F0243	Red retrobeads	Flattened tangential	Dorsomedial IC	0.03
F0259	FG	Flattened tangential	Rostromedial IC	0.02 (0.23)
F0260	FR	Flattened tangential	LN	0.06 (1.48)
F0247	Red retrobeads	Flattened tangential	Dorsomedial IC	0.16
F0235	Red retrobeads	Flattened tangential	LN	0.17
F0246	Red retrobeads	Flattened tangential	CN	1.10
F0255	Red retrobeads	Flattened tangential	Dorsomedial IC	0.16
	Green retrobeads		CN	0.43
F0258	FR	Flattened tangential	Rostral IC	0.01 (0.05)
	FG		LN	0.02 (0.06)
F0252	FR	Flattened tangential	MEG (15 kHz)	0.07 (1.02)
	BDA		MEG (1 kHz)	0.18 (1.39)
F0504	BDA	Flattened tangential	PEG	0.54 (6.09)
F0505	BDA	Flattened tangential	AEG	1.31 (7.13)
F0522	FR	Coronal	Large MEG	0.46 (22.02)
F0532	FR	Coronal	A1 (20 kHz)	0.22 (3.09)
	BDA		AAF (20 kHz)	0.04
F0533	BDA	Coronal	VP	0.01 (0.13)
F0535	FR	Coronal	AVF	0.14 (7.20)
	BDA		ADF	0.01
F0536	BDA	Coronal	A1 (2 kHz)	0.05 (0.39)

Note: Size of the IS in case F0061 was not calculated because several injections were made along 3 different IC penetrations

Tracer Injections in the Auditory Cortex

In the 8 animals that received cortical tracer injections, the EG was exposed by a craniotomy centered 17 mm anterior to the end of the skull. The tracers used were BDA and FR in 3 cases, BDA alone in 4 others, and FR alone in the last animal (Table 1 and Fig. 3*A*). The tracers were delivered by iontophoresis using the same parameters as in the IC injections, except the case with the single FR injection that was made by pressure with a microinjector. In the animals in which restricted injections were made in MEG (F0252, F0532, F0536; see Table 1 and Fig. 3*A*), we first recorded multiunit activity with the glass pipette in response to contralateral ear stimulation (for details, see Bizley and others 2005). Frequency response areas were constructed from the responses to pure tones (100 ms duration, presented pseudorandomly at a rate of 1 Hz from 500 Hz to 24 kHz in 1/3 octave steps and from 0 to 80 dB sound pressure level in 10 dB increments).

Histological Procedures

The animals were perfused transcardially 2–5 weeks after the initial surgery under terminal anesthesia with Euthatal (2 ml of 200 mg/ml of pentobarbital sodium; Merial Animal Health Ltd, Harlow, UK). The blood vessels were flushed with 300 ml of 0.9% saline followed by 1 L of fresh 4% paraformaldehyde in 0.1 M phosphate buffer (PB), pH 7.4. Each brain was dissected from the skull, maintained in the same fixative for several hours, and immersed in a 30% sucrose solution in 0.1 M PB for 3 days. In 8 cases with IC injections and 3 cases with injections in the cortex, the 2 hemispheres were dissected and gently flattened between 2 glass slides. In those cases, the cortex was later sectioned in a flat tangential plane and the rest of the brain in coronal sections. Eight other brains were sectioned in the standard coronal plane, and the remaining one was cut in the horizontal plane (Table 1). Sections (50 μm) were cut on a freezing microtome, and 6 sets of serial sections were collected in 0.1 M PB. One section in every 150 μm was used to analyze the tracer labeling.

In the 5 cases with retrobead injections, the sections were washed several times with 0.1 M PB, mounted on gelatinized slides, dried, and coverslipped with fluorescent mounting media. FR and FG were visualized with immunohistochemistry reactions, whereas BDA was

incubated in ABC (avidin biotin peroxidase, Vectastain Elite ABC Kit; Vector Laboratories, Burlingame, CA) only. Every step was carried out under gentle agitation. Sections were washed several times in 10 mM phosphate buffer saline (PBS) with 0.1% Triton X_{100} (PBS–Tx) and incubated overnight at +5 °C in the primary antibody (FR: antitetramethylrhodamine, rabbit IgG; Molecular Probes; dilution 1:6000. FG: rabbit anti-FG IgG; Chemicon International, Inc., Temecula, CA; dilution 1:2000). After rinsing 3 times in PBS–Tx, sections were incubated for 2 h in the biotinylated secondary antibody (biotinylated antirabbit IgG H + L, made in goat, dilution 1:200; Vector Laboratories). The sections were again rinsed several times in PBS–Tx and then incubated for 90 min in avidin biotin peroxidase (Vectastain Elite ABC kit; Vector Laboratories). Rinsing in PBS (without Tx) was followed by incubation in the chromogen solution with 3, 3′-Diaminobenzidine (DAB; Sigma-Aldrich Company Ltd, Dorset, UK). Sections were incubated in 0.4 mM DAB and 9.14 mM H_2O_2 in 0.1 M PB until the reaction product was visualized. When BDA and FR were visualized in the same tissue, the BDA was first reacted with ABC followed by DAB enhanced with 2.53 mM nickel ammonium sulfate. FR was reacted later with antibodies, a second ABC incubation, and DAB without nickel. In one case, F0258, 2 consecutive immunohistochemical reactions were carried out on the same sections, first enhanced with nickel and second without the use of heavy metals. Reactions were stopped by rinsing the sections several times in 0.1 M PB. Sections were mounted on gelatinized glass slides, air dried, dehydrated, and coverslipped.

In order to identify the different subdivisions of the IC and auditory cortex, one set of serial sections (1 every 300 μm) was counter stained with 0.2% cresyl violet, another set was selected to visualize cytochrome oxidase (CO) activity, and a third set was used to perform SMI_{32} immunohistochemistry. The border between the dorsal cortex (DC) and central nucleus (CN) of the IC was determined by applying the single-section rapid-Golgi method to coronal sections of the midbrain in one extra animal (for details, see Izzo and others 1987). CO staining was obtained after 12 h incubation with 4% sucrose, 0.025% Cytochrome C (Sigma-Aldrich), and 0.05% DAB in 0.1 M PB at +37 °C. To stain neurofilament H in neurons, we used monoclonal mouse anti-SMI_{32} (dilution 1:4000; Sternberg Monoclonals, Inc., Latherville, MA). After immersion for 60 min in a blocking serum solution with 5% normal horse serum, the sections were incubated overnight at +5 °C with the mouse antibody and 2% normal horse serum in 10 mM PBS. Anti-mouse biotinylated secondary antibody (mouse ABC kit, dilution 1:200 in PBS with 2% normal horse serum; Vector Laboratories) was used after brief washings in 10 mM PBS. Immunoreaction was followed by several more washings in PBS, incubation in ABC, and visualization using DAB with nickel–cobalt intensification (Adams 1981; J. A. Winer, personal communication).

Histological analysis was carried out, and drawings made with a Leica DMR microscope with filters for fluorescence (530 nm light emission for red retrobeads and FR, and 460 nm for green retrobeads) and a digital Leica camera using TWAIN software (Leica Microsystems, Heerbrugg, Switzerland). Histological reconstructions and morphometric analysis were performed using Neurolucida software (Microbright Field Corp., Williston, VT). Statistical comparison of morphometrical measures was carried out using SPSS software (SPSS Inc., Chicago, IL).

Results

Cytoarchitecture of the EG

The EG is delimited by the suprasylvian sulcus (*sss*) and displays a distinct cytoarchitectonic pattern in its anterior, middle, and posterior regions (Figs 1 and 2). The MEG forms the dorsal part of the gyrus and has a koniocortical pattern characteristic of primary cortices. Its supragranular layers contained heavy Nissl and CO staining (Figs 1*F* and 2*A*,*D*), whereas large intensely stained neurons were found in layer V (Fig. 2*A*,*D*, arrows). CO and SMI_{32} staining formed a complementary pattern, with layer IV heavily positive for CO and negative for SMI_{32} (Figs 1*B*,*D*,*F* and 2*D*,*G*). Pyramidal cells in the lower part of layer III and upper part of layer V were intensely positive for SMI_{32}, giving rise to a clear bilaminar appearance (Figs 1*B*,*D* and 2*G*). This distinctive pattern in the MEG enabled us to define borders with the AEG and PEG in both coronal and tangential sections (Fig. 1*B*,*D*,*F*, thin arrows).

The size of the immunopositive SMI_{32} cell bodies in layer V was measured on flattened tangential sections across MEG. The positive cells tended to be smaller toward the anterior part of the MEG where AAF has been described (Kowalski and others 1995; Bizley and others 2005). However, no significant differences were found when 2 sets of neurons (n = 465) from the most anterior and posterior part of the MEG were compared (mean soma area 381 ± 129 vs. 433 ± 151 μm^2, respectively).

The PEG is bordered dorsally by the MEG (Fig. 1*B*,*D*,*F*, thin arrows), rostrally by the pseudosylvian sulcus (*pss*), and caudally by the posterior part of the *sss* (Fig. 1*B*–*F*). This region has a cytoarchitectonic pattern characteristic of secondary cortices. Nissl staining revealed a less granular appearance in the upper layers of the PEG and small cell bodies in layers V and VI (Fig. 2*C*). CO staining was homogenous and less dense than in the MEG (Figs 1*E*,*F* and 2*F*), whereas SMI_{32} immunostaining in the PEG was found mainly in large pyramidal neurons in layer V (Figs 1*C*,*D* and 2*I*). Some differences could be observed between the anterior and posterior parts of the PEG. CO staining was stronger in the anterior region, adjacent to the *pss*, than in the posterior region (Fig. 1, compare PEG in *E* and *F*). A more conspicuous pattern of Nissl staining was apparent in anterior PEG, although layer VI seemed to be thinner and more darkly stained in the posterior part (not shown). Moving ventrally within the PEG, layer V SMI_{32}-positive neurons became smaller and less abundant (Fig. 1*B*,*C*, arrowheads), whereas CO staining became weaker. The ventral PEG borders the rhinal cortex, which contained no discernible SMI_{32} or CO staining (Fig. 1*B*).

The AEG is bordered dorsally and ventrally by the *sss* and *pss*, respectively (Fig. 1*A*–*C*,*E*). CO staining was heavy in the upper cortical layers and homogeneous within those layers but was much weaker in the *pss* (Figs 1*E* and 2*E*). SMI_{32}-positive neurons formed a bilaminar pattern that was quite similar to that in the MEG but with fewer positive elements in layer III (compare Fig. 2*G*,*H*). A distinct pattern of immunostaining was apparent in the more anterior and ventral part of the AEG, with very large SMI_{32}-positive pyramidal cells in layer V and SMI_{32}-positive dendritic elements in the supragranular layers (Fig. 1*B*, empty arrow). With Nissl staining, this most anterior part of AEG exhibited a more granular pattern in layers II–IV (not shown).

Origin of the Auditory Corticocollicular Projection

A summary of different tracer injections made in the auditory cortex and in the IC is shown in Figure 3 and Table 1. Using both anterograde tracers injected at the origin of the projection and retrograde tracers in the target allowed us to define the morphology and topography of the neurons in the auditory cortex and of their terminal fields in the IC. In 20 animals, a total of 11 tracer injections were made in the auditory cortex and 14 in the IC (Fig. 3), together with multiple IC injections in case F0061. Tracer injections were made into each of the main subdivisions of the auditory cortex (MEG, AEG, and PEG) in at least 2 animals. In the MEG, a total of 6 tracer injections were made in different locations (Fig. 3*A*). The IC injections covered every subdivision of this midbrain nucleus (Fig. 3*B*–*D*), and the findings presented are the most representative for each.

The most representative cases in which tracer injections were made in the IC (Figs 4–7) and in the auditory cortex (Figs 8–11) were chosen to illustrate the results. The amount of

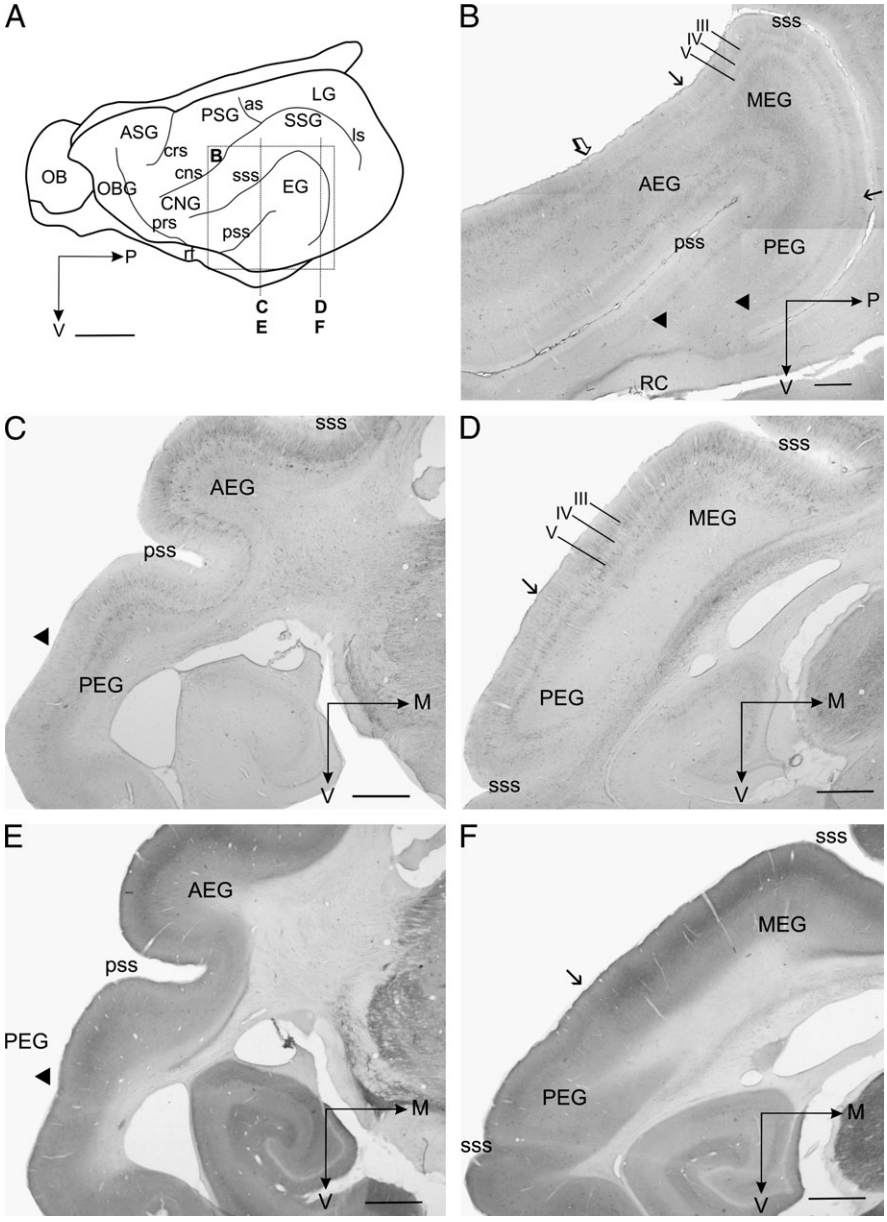

Figure 1. (*A*) Lateral view of the ferret brain showing the different gyri and sulci in the cortex. The ferret auditory cortex is located in the EG. The square in (*A*) indicates the area shown at higher magnification in (*B*); vertical lines (CE, DF) depict the level and plane of sections shown in (*C–F*). (*B*) Section cut tangentially, flattened, and immunostained with the SMI_{32} antibody. A bilaminar pattern of staining is prominent in the primary region in the MEG, less so in the AEG, and is absent in the PEG. Thin arrows indicate borders between MEG and AEG/PEG. The most anterior part of the AEG is characterized by intense staining in layer II/III (empty arrow marks the posterior limit of this). In the most ventral part of the PEG, SMI_{32} immunoreactivity was almost absent (below arrowheads). (*C*, *D*) Sections cut in the coronal plane and stained with the SMI_{32} antibody. In (*C*), the bilaminar pattern in AEG is transformed to a monolaminar pattern in dorsal PEG, which disappears in ventral PEG (as indicated by the arrowhead). (*E*, *F*) Sections cut in the coronal plane and stained for CO. In (*E*), PEG is weakly stained for CO, whereas in AEG the staining is strong and uniform in the supragranular layers. In PEG, the most ventral region is more weakly stained than the dorsal region (arrowhead). In (*F*), robust staining of layer IV is characteristic of MEG (arrow indicates the border between MEG and PEG). Scale bar is 5 mm in (*A*) and 1 mm in (*B–F*). ASG, anterior sigmoid gyrus; *as*, ansinate sulcus; CNG, coronal gyrus; *cns*, coronal sulcus; *crs*, cruciate sulcus; LG, lateral gyrus; *ls*, lateral sulcus; M, medial; OB, olfactory bulb; OBG, orbital gyrus; P, posterior; *prs*, presylvian sulcus; PSG, posterior sigmoid gyrus; RC, rhinal cortex; *rf*, rhinal fissure; SSG, suprasylvian gyrus; V, ventral.

tracer diffusion from the ISs varied according to the tracer used. No diffusion occurred with the retrobeads, whereas the FR ISs were surrounded by a large halo (Fig. 3 and Table 1). The size of the ISs also varied depending on both the parameters of the injections (pressure or iontophoresis, micropipette tip size, injection times, etc, see Materials and Methods) and the density of the neuropil at the IS. Although this prevented us from making quantitative comparisons of the projections arising from different ISs, the use of different tracers avoided the limitations associated with any particular one and allowed us to inject 2 tracers in particular regions of IC or auditory cortex. In order to compare the corticocollicular projection arising from different areas of the auditory cortex in the same animal, a combination of FR and BDA was used. FG and retrobeads were injected into the IC in order to obtain exclusively retrograde labeling. Because there is no diffusion from the ISs, retrobeads were also used to obtain restricted injections at particular locations (Fig. 3 and Table 1).

Animal F0061 (Table 1) is a representative case in which large tracer injections were made in the midbrain. In this animal, 2 or

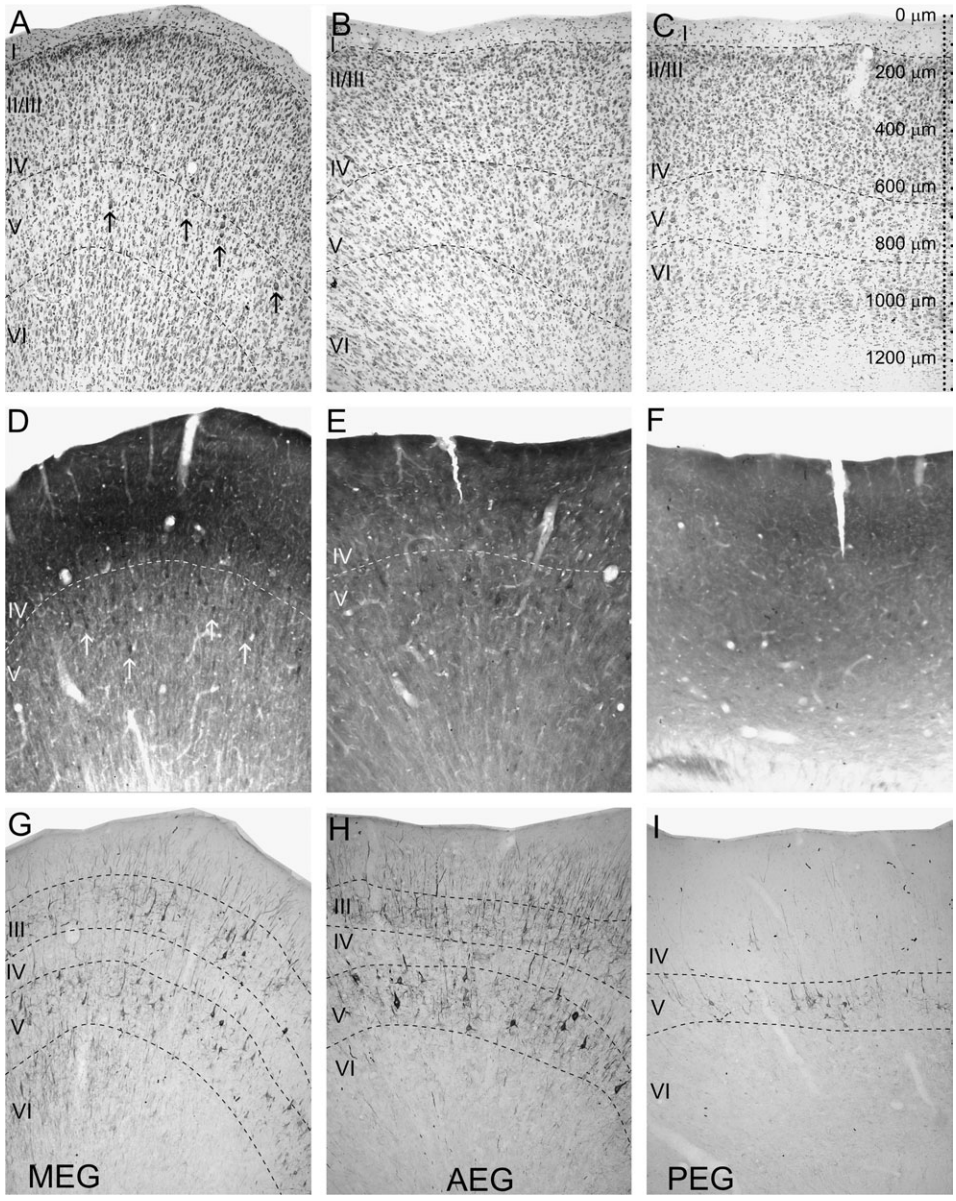

Figure 2. Cytoarchitectonic features observed in the MEG, AEG, and PEG. Figures from MEG, AEG, and PEG are organized in 3 columns to show Nissl (*A–C*), CO (*D–F*), and SMI_{32} antibody staining (*G–I*) in different rows. With Nissl staining, cell density is highest and the granular appearance of the supragranular layers strongest in MEG (*A*), weakest in PEG (*C*), and intermediate in AEG (*B*). CO staining is strongest in the supragranular layers, although some CO-positive layer V neurons can also be observed (arrows). The supragranular CO staining is strong in MEG (*D*), intermediate in AEG (*E*), and weak in the PEG (*F*). Immunostaining with the SMI_{32} neurofilament antibody reveals a bilaminar pattern in MEG (*G*) and AEG (*H*), whereas in PEG there is only a monolaminar pattern of layer V positive neurons (*I*). The dashed lines indicate the borders of the different cortical layers, which were determined on the basis of the Nissl, CO, and SMI_{32} staining. Scale is shown in (*C*).

3 FR injections were made in each of the 3 dorsoventral penetrations at different lateromedial locations within the IC. The tracer spread from the ISs to cover the entire IC, reaching the periaqueductal gray (PAG) medially, the fibers of the brachium and the deep layers of the superior colliculus (SC) rostrally, and the cuneiform nucleus (Cu) ventrally.

Retrogradely labeled neurons were observed in every region of the ipsilateral EG in this animal (Fig. 4). These neurons formed a continuous band of labeling in the gyrus that extended into the *sss*. In the anterior *sss*, labeled neurons were observed in the anterior and posterior banks of the sulcus, although they were less numerous in its anterior bank (Fig. 4*B–D*). In the posterior *sss*, labeled neurons were also observed in both anterior and posterior banks but were less numerous in the posterior bank (Fig. 4*B*–D). As in the *sss*, labeled neurons formed a continuous band in both banks of the *pss*, thereby continuing the labeling found in AEG and PEG (Fig. 4*D–H*). Labeling was found in the most ventral part of the PEG, beyond the *sss*, but stopped before the rhinal fissure (Fig. 4*H*). The somata of the labeled neurons were located in layer V and their apical dendrites extended radially to the pial surface. Labeled apical dendrites were observed in every part of the EG but more frequently in MEG and PEG (Fig. 4).

Labeled neurons were also observed in corresponding regions of the contralateral EG but were much less numerous (not shown).

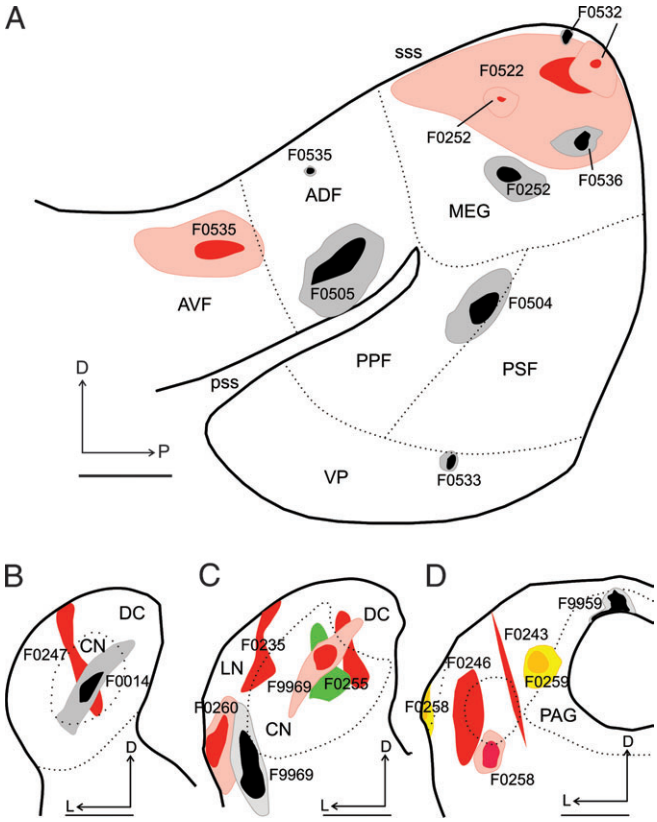

Figure 3. Drawings showing the location and size of the tracer ISs in the auditory cortex (*A*) and in the IC (*B–D*) of all the animals (except F0061) used in this study. The EG is shown in a lateral view (*A*) and the IC is shown at 3 different coronal levels from caudal (*B*) to rostral (*D*). The red color range was chosen to illustrate FR and Red Retrobead ISs, the yellow range for FG, and gray–black for BDA. Green Retrobead ISs are indicated by the green area. A center and a halo in the IS could be distinguished when FG, FR, and BDA were used and are illustrated using dark and light color ranges. No halo was present with the Retrobead injections because no tracer diffusion occurs with this tracer. Because multiple tracer injections were made in case F0061, its ISs are not included in this figure. Scale bars represent 2 mm in (*A*) and 1 mm in (*B–D*). D, dorsal; L, lateral; P, posterior.

Neuronal Morphology

The neurons labeled in the auditory cortex after IC injections were always medium and large size pyramidal cells with triangular bodies located in layer V. However, the morphology of the dendritic ramification could be observed only when large or multiple injections were made in the IC (e.g., in Figs 4 and 5, case F0061). These neurons had 3–6 basal dendrites with dendritic fields generally oriented parallel to the cortical layers (Fig. 5*B,D–G*). The apical dendrite ran perpendicular to the layers, giving rise to secondary dendrites along its trajectory (Fig. 5*D*) and ending after several ramifications in layers I–II (Fig. 5*J–L*). Several features of the labeled neurons differed depending on their location in the EG. The dendritic arborizations were profuse in the MEG, but less so in the PEG, and even less in the AEG (compare Fig. 5*A,B,C*). By contrast, in general, the basal dendrites of the labeled neurons in the AEG did not follow the laminar organization of the cortex (Fig. 5*B,E*). Dendritic ramifications of the apical dendrites in layers I–II were very numerous in the PEG, less so in the MEG, and infrequent in the AEG (Figs 4 and 5*J–L*). However, the ramifications of the apical dendrites themselves were more profuse in AEG than in the other regions (compare Fig. 5*K* with Fig. 5*J,L*).

Because entire filling of the dendritic trees was not observed, no morphometric analysis of the dendritic arborization was carried out. We did, however, measure the soma size of the neurons in which the proximal dendrites were also filled (so that we could be certain that the entire soma was filled), allowing us to make comparisons across the 3 different regions of the auditory cortex. This morphometric analysis revealed that the largest labeled cell bodies were found in the AEG, the smallest in the PEG, with those located in the MEG being of intermediate size (analysis of variance [ANOVA], $P \leqslant 0.001$, Table 2). However, post hoc tests (Dunnett's *t*-test for multiple comparisons) showed that significant differences in soma size were present only between the neurons located in the AEG and each of the other areas (Table 2).

Distribution of the Cortical Projection in the IC

To study the topographic organization of the corticocollicular projection, restricted injections were placed in different subdivisions of the IC (Figs 3*B–D*, 6, and 7) and the auditory cortex (Figs 3*A* and 8–11, see also Table 1). The IC injections were used to explore the location of retrogradely labeled neurons in the cortex, whereas injections of anterograde tracer in auditory cortex allowed us to observe the location and morphology of terminal fields in the IC.

We identified the border between the CN and the DC using the following criteria. First, recordings in ferret IC show a prominent CN, covering the region that we have labeled here as CN (Moore and others 1983). Second, we found that CO staining is very dense in the CN and much less so in DC. Third, we confirmed our definition of ferret CN with fast Golgi staining, on the basis of the location of disc-shaped neurons with laminar-oriented dendritic fields. The relative location of these subdivisions of the ferret auditory midbrain is also consistent with that proposed by other authors for this species (Fuentes-Santamaria and others 2003; Henkel and others 2003).

When the IS in the IC was located in its dorsomedial region, including both the DC and the dorsal part of the CN (Fig. 6*A*), retrograde labeling was observed across the EG, although more extensively in MEG and PEG than in AEG (Fig. 6*C*). Neurons were located predominantly in layer V, with a small number occurring deeper in layer VI. This was most evident in PEG (Fig. 6*C*, section i and j). In AEG, neurons were concentrated in the posterior part (Fig. 6*C*, sections e–k), with almost no labeled cells in the anterior half of this gyrus (Fig. 6*C*, sections a–d). In PEG, neurons were found across the whole extension of the gyrus, including its most ventroanterior part (Fig. 6*C*, section f).

Tracer injections located in the lateral nucleus (LN) of the IC, resulted in a distinct pattern of labeling in the auditory cortex with many labeled cells in the PEG, relatively few in the MEG, particularly in caudal MEG where A1 is found, and almost none in the AEG (Fig. 7*A*). When the injection site was located in the CN, most of the labeled neurons were located in the MEG, with some in both PEG and AEG (Fig. 7*B*). The more extensive retrograde labeling shown in Figure 6 therefore results from inclusion of the DC in the IS.

Tracer injections in the MEG always gave rise to labeled terminal fibers and boutons in the dorsomedial region of the IC bilaterally and in the LN ipsilateral to the cortex injected (Figs 8 and 9). Within the LN, a network of fibers was present in layer 2, which included many terminals and *en passant* boutons (Fig. 8*B,E*). The terminal fields in the dorsomedial IC were more

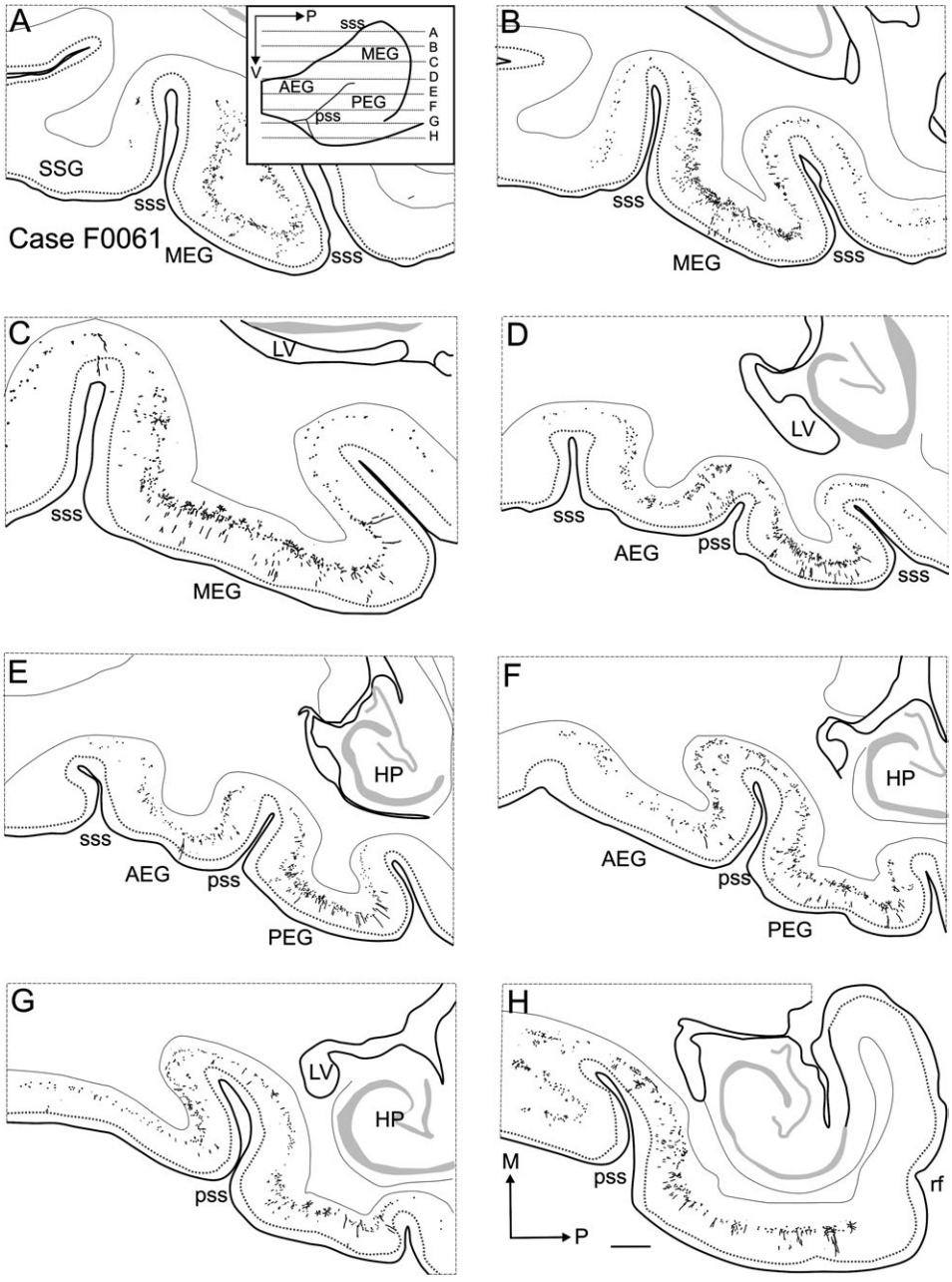

Figure 4. Location of cortical neurons that form the descending projection to the midbrain. Multiple FR injections in the ipsilateral IC (case F0061) retrogradely labeled neurons in layer V across the entire extent of the EG, including both *sss* and *pss*. The drawings show the labeling of cellular bodies and apical dendrites at different dorsoventral levels of the EG, as schematized in the inset in (*A*). Scale bar in (*H*) is 1 mm. HP, hippocampus; LV, lateral ventricle; M, medial; P, posterior; *rf*, rhinal fissure; SSG, suprasylvian gyrus; V, ventral.

profuse in the DC than in the dorsal part of the CN (Fig. 8*C* and 9*B,C*). The terminal fields located in the latter region had the same orientation as the fibrodendritic laminae that have been described for the CN in other species (reviewed in Oliver 2005). In general, the labeled axons were thinner and their terminals smaller, with less bouton density, than those in the DC (Fig. 8*C–E*, arrows). The terminal labeling in the CN and DC could clearly be distinguished by the different orientation of the labeled fibers in these structures (Fig. 8*C*). When the halo of the IS spread across the MEG from a narrow center (Fig. 8, case F0522), a main band of terminal labeling was observed in the center of the CN, with other more lightly labeled bands in the same subdivision of the IC (Fig. 8*C,E*).

By making a series of small tracer injections in restricted regions of the MEG in different ferrets (Fig. 3*A*), we were able to show that the location of the terminal fields in the CN varied topographically with the location of the IS in the MEG. The most representative case is F0252, in which 2 different tracers were injected at different dorsoventral locations in the MEG (Fig. 9; see also Fig. 3*A* and Table 1). The tracers used were FR in the dorsal part of the MEG and BDA in the ventral part (Fig. 9*D*). Electrophysiological recordings were made prior to each tracer injection in this animal, and the best frequencies were 1 and 15 kHz at the BDA and FR ISs, respectively. These ISs were restricted with no tracer spread to the other tracer IS or beyond the limits of MEG (Figs 3*A* and 9*D*). The bands of

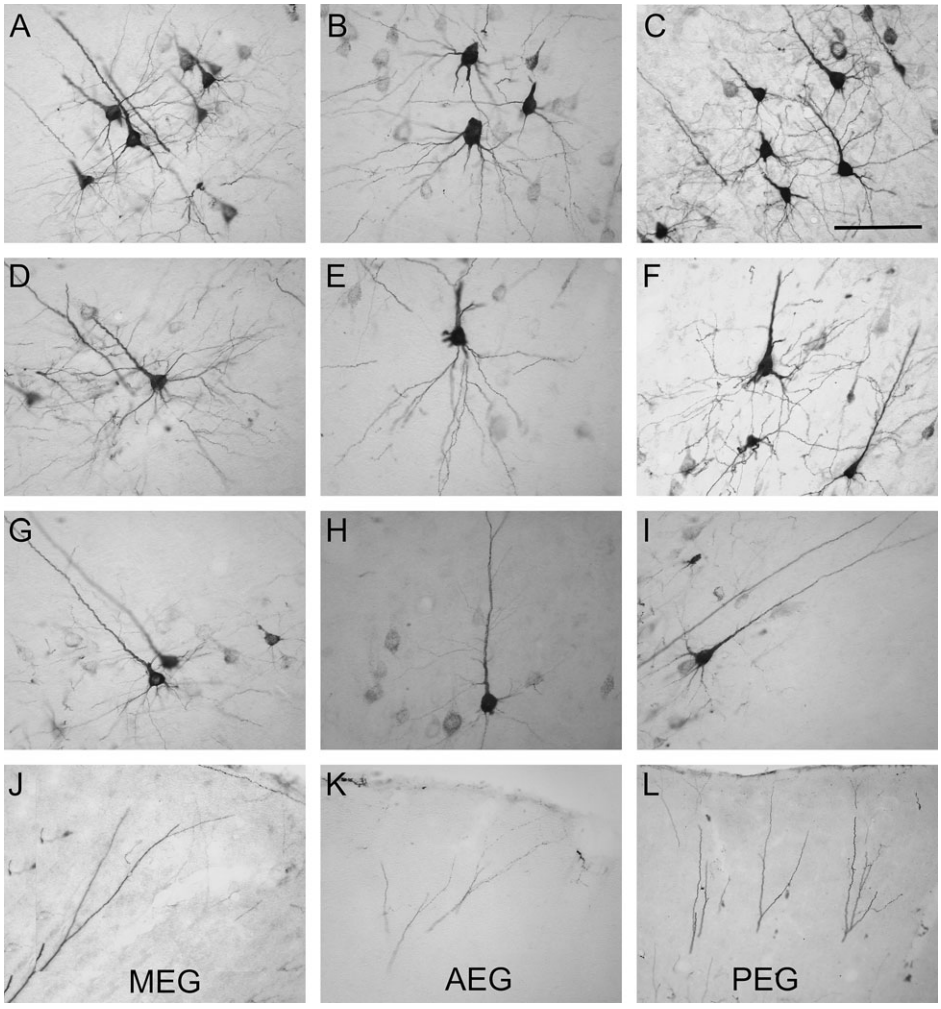

Figure 5. Morphology of the cortical neurons projecting to the IC. Left column (*A*, *D*, *G*, *J*) shows neurons located in the MEG, middle column (*B*, *E*, *H*, *K*) in the AEG, and right column (*C*, *F*, *I*, *L*) in the PEG. Every neuron comes from animal F0061. In all cases, the labeled apical dendrite is oriented perpendicular to the white matter and toward the pial surface. Scale bar in (*C*) is 100 μm.

terminal labeling in the CN were located dorsolaterally following the BDA injection and ventromedially for the FR injection (Fig. 9*B*,*C*). The features of the labeled terminal fibers were consistent with those described above for larger cortical injections, although with such small ISs, the amount of terminal labeling was relatively small and boutons were difficult to visualize (Fig. 9*E*,*F*, arrows). Irrespective of the location of the IS in the MEG, we never observed labeled terminal fields in the ventrolateral part of the CN.

Tracer injections in the PEG (Fig. 10, case F0504) resulted in terminal fields in the IC that were similar to those found following MEG injections, with the exception that no terminals were observed in the CN. The labeling in the ipsilateral LN was located in layer 2 and spread along its dorsoventral dimension (Fig. 10*A*–*D*). The morphology of the terminal fields was similar to that observed following MEG tracer injections. In contrast, the terminal fields observed in the DC displayed a more intricate pattern, combining thick and thin fibers with many *en passant* boutons (Fig. 10*F*,*G*, arrows). Although not shown, the location and morphology of the terminal fields in the IC was the same when the tracer injection was located in the ventroposterior (VP) area of the PEG (Fig. 3*B*, case F0533).

A totally different pattern of terminal labeling was found when tracer injections were located in the AEG (Fig. 11, case F0505). Terminals were absent from the CN and DC, and the main terminal fields were concentrated in the PAG and the tegmental areas surrounding the IC, including the Cu, the ventral border of the IC, the sagulum, the perilemniscal regions close to the pontine nuclei, the intercollicular commissure, and the deep layers of the SC (Fig. 11). Some terminal fibers and boutons were observed in the ipsilateral LN, but these were less numerous and their location more ventral than in the cases where the ISs were located in MEG or PEG (Fig. 11*C*,*D*). The other cases with injections in the AEG produced the same pattern of labeling as that shown in Figure 11, apart from minor differences in the amount of labeling observed in the PAG.

Discussion

In this study, we examined the cytoarchitectonic features of the ferret auditory cortex and the organization of its descending projections to the IC. In conjunction with previous functional data (Nelken and others 2004; Bizley and others 2005), these results provide valuable insights into the organization of the

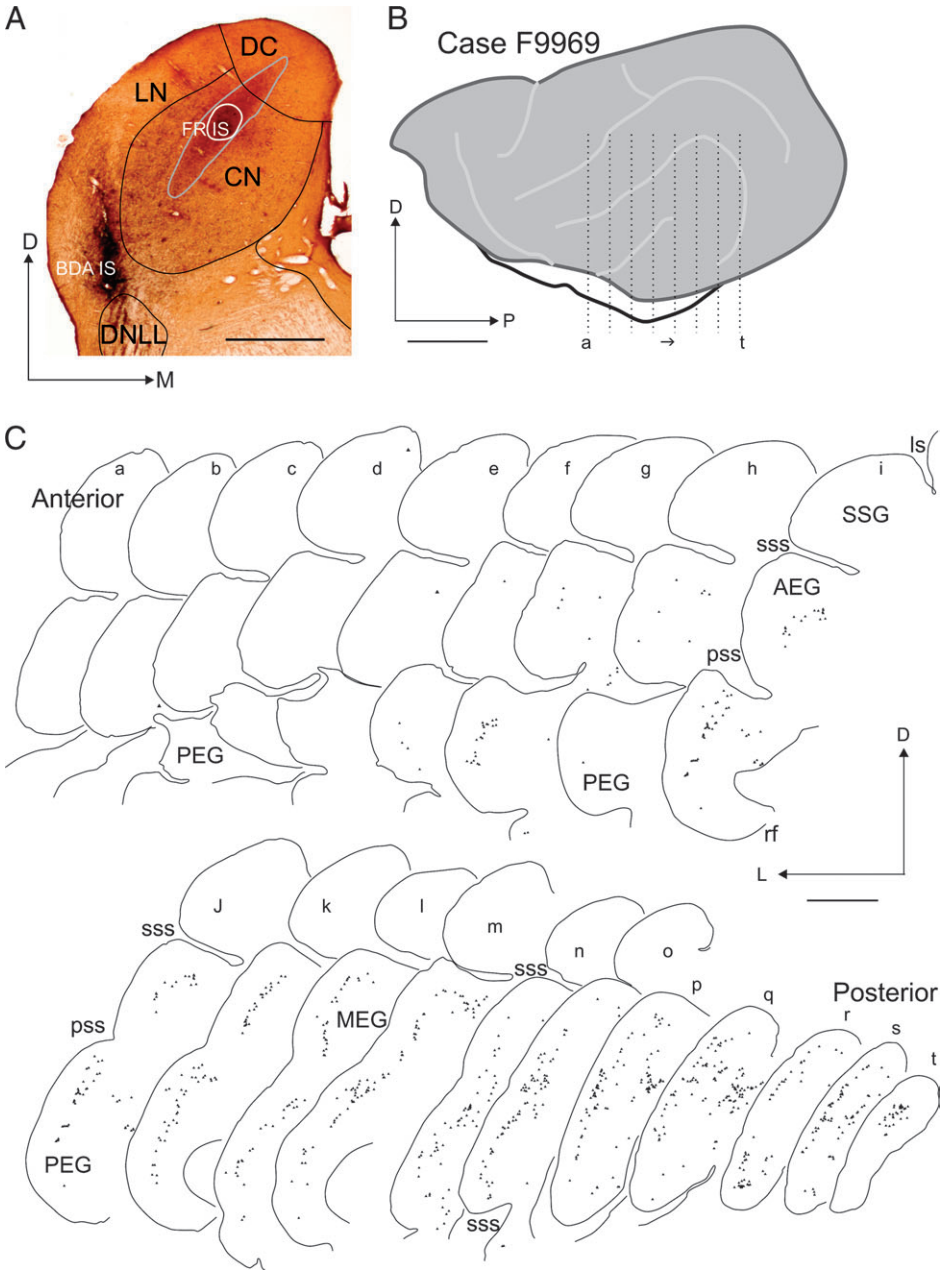

Figure 6. Location of cortical cells retrogradely labeled by a restricted FR injection in the IC (case F9969). The IS (*A*) is centered in the middle of the CN, and the tracer spread following the dorsomedial to ventrolateral laminar orientation of the nucleus to reach the DC. Labeled cells are located mainly in the MEG and PEG and are less frequent in the AEG. This is shown in (*C*) on coronal sections taken at the rostrocaudal levels indicated in (*B*). A BDA injection is also located in the LN (*A*), which produced labeling equivalent to that shown in Figure 7 for a different LN injection. For clarity, however, no retrogradely labeled BDA cells are illustrated here. Scale bar is 1 mm in (*A*), 5 mm in (*B*), and 2 mm in (*C*). D, dorsal; DNLL, dorsal nucleus of the lateral lemniscus; L, lateral; l.s. lateral sulcus; M, medial; P, posterior; *rf*, rhinal fissure; SSG, suprasylvian gyrus.

auditory cortex in a species that is becoming increasingly popular for studies of sensory processing and plasticity. Figure 12 presents a summary of the different auditory cortical regions and fields that have been described in the ferret, together with their descending projections to the IC. We have shown that 3 different regions, MEG, PEG, and AEG, can be differentiated on the basis of Nissl, CO, and SMI_{32} staining in the EG, which correspond to the auditory areas revealed by sound-evoked 2-deoxyglucose labeling (Wallace and others 1997). Our results also show that each of these cortical regions has a different pattern of descending projections. The only projections from auditory cortex to the CN of the IC arise from the MEG, whereas only AEG neurons innervate pericollicular structures (Fig. 12). In contrast, inputs to the ipsilateral LN are a common feature of all regions in the EG, although projections from the MEG and PEG differ in their strength and terminal location from those originating in the AEG. Distinct patterns of corticocortical (Bizley and others 2006) and corticothalamic (Nodal and others 2006) projections have also recently been described for each region of the EG, further suggesting that they have different roles in auditory processing.

Electrophysiological data indicate that these regions can be further subdivided into separate cortical fields (Bizley and others 2005). It is therefore important to consider whether

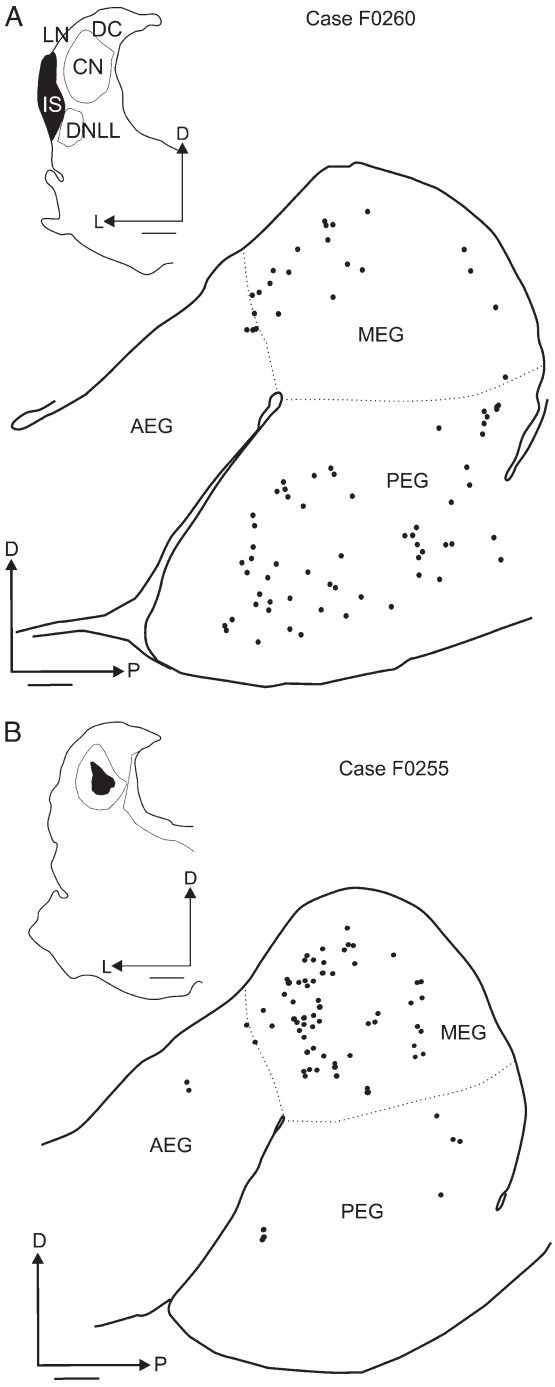

Figure 7. Examples showing the distribution of cortical cells labeled retrogradely by restricted tracer injections in the IC. In (*A*) (case F0260), an FR IS is located in the LN, spreading ventrally to the nucleus of the sagulum (Sag). Labeled cells in the ipsilateral EG are located mainly in the PEG and MEG, with virtually none in the AEG. In (*B*) (case F0255), an injection of green retrobeads was made in the CN, and most of the labeled cells are restricted to the MEG. Dot lines indicate the limits of the MEG. The EG was reconstructed from flattened horizontal sections taken every 300 μm. Scale bars represent 1 mm. D, dorsal; DNLL, dorsal nucleus of the lateral lemniscus; L, lateral; P, posterior.

the results of the present study support these functional subdivisions. The best-described fields are cortical areas A1 and AAF in the MEG. These primary fields have been the subjects of numerous electrophysiological (Kowalski and others 1995; Depireux and others 2001; Fritz and others 2003, 2005; Elhilali and others 2004; Bizley and others 2005; Mrsic-Flogel and others 2005) and optical imaging studies (Versnel and others 2002; Nelken and others 2004; Mrsic-Flogel and others 2006). According to these studies, A1 and AAF both have tonotopic axes that are arranged in an approximately dorsal-to-ventral direction, with the highest sound frequencies represented at the dorsal tip of the gyrus. Neurons in AAF are characterized by shorter response latencies than those in A1 and an under representation of midfrequencies (Bizley and others 2005). Nevertheless, because of the similarity of their tonotopic gradients, defining the border between these fields is not straightforward. Although we found no clear cytoarchitectonic differences within the MEG, SMI_{32}-positive neurons in layer V tended to be smaller in the anterior region corresponding to where AAF is thought to be located. In the cat, SMI_{32} immunostaining of dendritic arborizations in layers V and VI has been reported to be indicative of AAF (Mellot and others 2005). We also found numerous SMI_{32} immunostained dendritic elements in the ferret but only on the anterior bank of the *sss*. This is where Kowalski and others (1995) proposed the low-frequency region of AAF to be located.

Previous studies suggest that there may be 3 different fields in the PEG. Based on a reversal in their rostral-to-caudal tonotopic gradients in the middle of the PEG, Bizley and others (2005) described 2 fields, the posterior pseudosylvian field (PPF) and the posterior suprasylvian field (PSF). These fields correspond in location to the area referred to as secondary auditory field (A2) by Pallas and Sur (1993), who also described a VP area, lying ventral to A2. The variations that we observed in Nissl, CO, and SMI_{32} staining (Fig. 1) are consistent with the existence of 3 different areas within the PEG.

Three different fields have also been described in ferret AEG. Manger and others (2002, 2004, 2005) reported that the anterior ectosylvian sulcal cortex (area AES) is located on the ventral bank of AEG where it extends into the *pss* and that this region is innervated by visual cortex. The multisensory nature of this area was further highlighted by Ramsay and Meredith (2004) by combining tracer injections in the somatosensory and visual cortices. Auditory responses have been revealed throughout the AEG by intrinsic optical imaging (Nelken and others 2004) and subsequently by more detailed electrophysiological mapping (Bizley and others 2005). The latter study identified 2 fields, the anterior dorsal field (ADF) and, more ventrally, the anterior ventral field (AVF). Our results suggest that the pattern of the SMI_{32} immunostaining (Fig. 1) can also be used to some extent to distinguish different regions within the AEG. The most ventral and anterior part of the AEG, corresponding to AVF, which contains neurons that respond more robustly to noise than to tones, is characterized by a granular pattern of Nissl staining and dendritic elements in the supragranular layers that are strongly positive for SMI_{32}. This cytoarchitectonic pattern resembles that of insular cortex in the cat (Clascá and others 1997).

Our cytoarchitectonic data are therefore consistent with some of the physiological subdivisions that have been documented in the ferret EG. A combination of electrophysiological mapping and discrete tracer injections in each of the regions so far identified is now required to confirm and extend these findings according to differences and similarities in the response properties and connectivity of the neurons found there. This is essential for future studies of auditory processing and plasticity in this species.

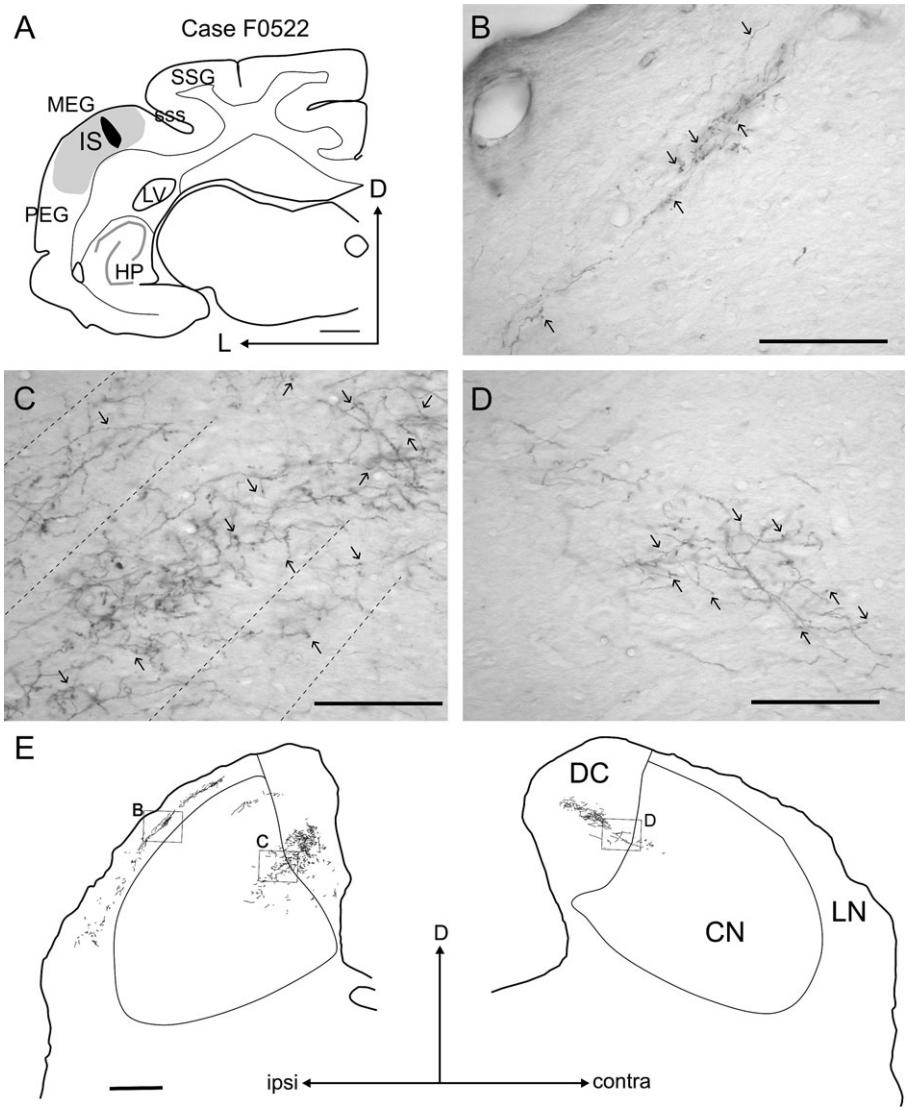

Figure 8. Anterograde labeling in the IC observed after an injection of FR in the MEG. In (*A*), the IS is shown in a coronal section at the level of the left MEG. The halo of the IS spread along the MEG. Examples of labeled terminal fields in the ipsilateral LN and CN and in the contralateral CN are shown in (*B*), (*C*), and (*D*). The terminal fields have a distinctive orientation in every IC subdivision. Details of the terminal fields in the CN are shown in (*C*) and (*D*), ipsilateral and contralateral to the IS, respectively. Arrows indicate terminal boutons and the dashed lines in (*C*) the orientation of the terminal fields in the CN. A drawing at the level of the center of both ICs is shown in (*E*), illustrating the distribution of the terminal fields. Scale bars represent 1 mm in (*A*), 100 μm in (*B–D*), and 500 μm in (*E*). contra, contralateral; D, dorsal; HP, hippocampus; ipsi, ipsilateral; L, lateral; LV, lateral ventricle; SSG, suprasylvian gyrus.

Comparisons with the Cat Auditory Cortex

In auditory research, the cat is the closest species to the ferret, and the different fields comprising its auditory cortex have been defined both anatomically and functionally (for review, see Winer and others 2005; but also Tsytsarev and others 2004; Lee and Winer 2005). In the cat, a total of 11 auditory cortical fields have been described. At present, it appears that the ferret auditory cortex can be subdivided into 8 different areas, although it seems likely that this number will rise in the future, particularly as the sulcal regions are investigated in more detail.

More important than their number is the ability to identify homologies between the fields that have been identified in different species. The 2 primary fields in MEG constitute the core auditory cortex and are clearly equivalent to cat A1 and AAF. Comparison of the present results with data from the cat reveals a marked similarity in both the cytoarchitectonic features of the core fields (Winer 1992; Mellott and others 2005) and in the organization of their corticocollicular projections (compare Figs 8 and 9 with Figs 3 and 4 in Winer and others 1998). In both species, these projections end in the LN ipsilaterally and in the dorsomedial IC bilaterally. The most intriguing interspecies difference is that A1 and AAF share a common tonotopic axis in the ferret (Bizley and others 2005), whereas they exhibit opposing tonotopic gradients that meet at a high-frequency border in the cat and other mammalian species (reviewed by Winer and others 2005). However, interspecies variations of this sort are not rare, for example, A1 is the more anterior primary field in guinea pig (Redies and others 1989; Wallace and others 2000), whereas the primary fields share a low-frequency border in the macaque (Merzenich and Brugge 1973).

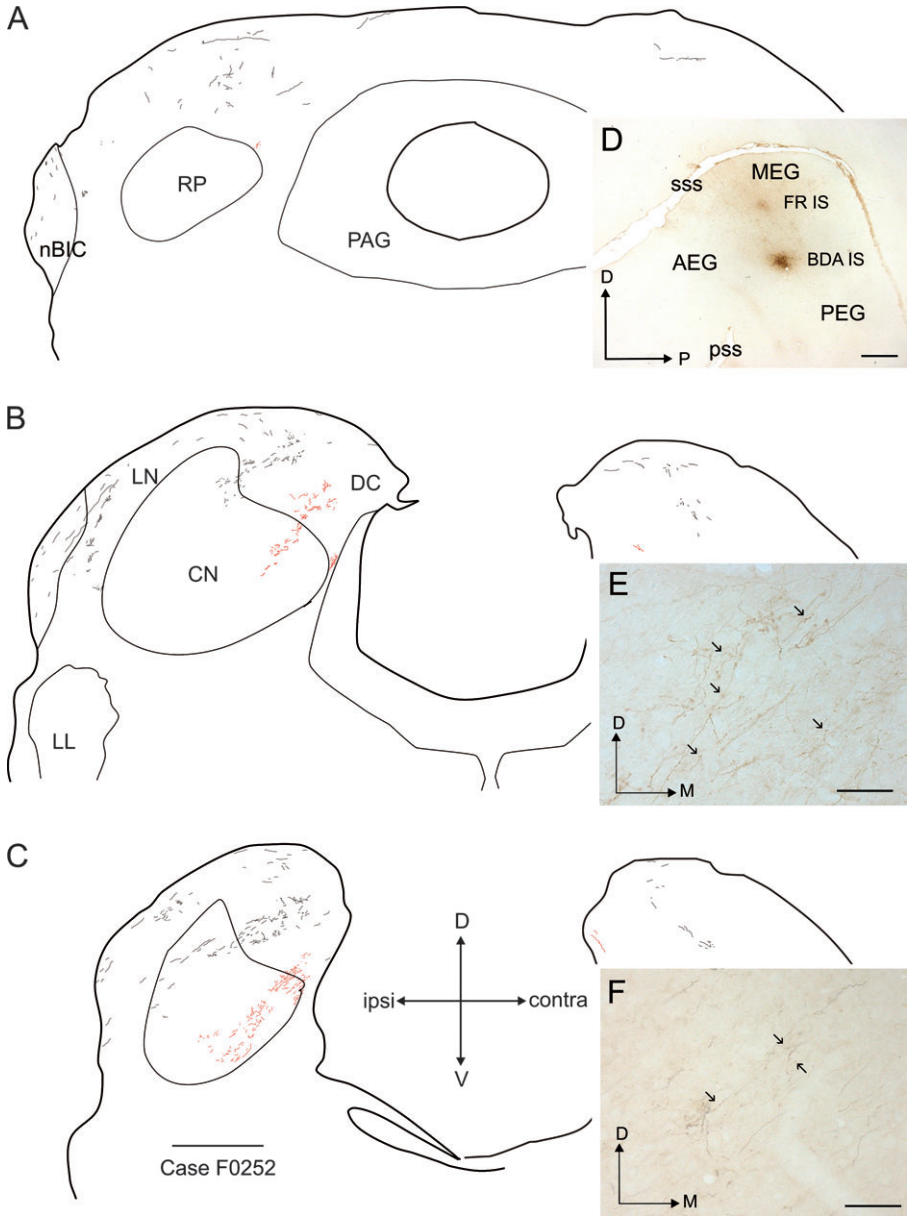

Figure 9. Anterograde labeling in the IC observed after 2 restricted tracer injections located in the MEG. FR and BDA were injected in the dorsal and ventral part of the MEG, respectively (*D*). Drawings at different IC rostrocaudal levels (*A–C*) show terminal fields in the 3 subdivisions of the ipsilateral IC. The contralateral labeling is much weaker and appears to show a similar pattern. The location of the terminal fields in the IC is related to the IS in the MEG. FR terminal fields are drawn in red, and BDA terminal fields in black. Details of red and black terminals are shown in (*E*) and (*F*), respectively, with arrows pointing at labeled terminals. Scale bar in (*A–D*) is 1 mm and in (*E*) and (*F*) is 50 µm. contra, contralateral; D, dorsal; ipsi, ipsilateral; LL, lateral lemniscus; M, medial; nBIC, nucleus of the brachium of the inferior colliculus; P, posterior; RP, rostral pole of the inferior colliculus; V, ventral.

Based on their anatomical locations, it is tempting to equate the PPF, as defined by Bizley and others (2005), with A2 in cat, PSF with the cat posterior auditory field (PAF), and VP with the ventroposterior auditory field. Moreover, the pattern of SMI_{32} staining in these regions of the ferret PEG is similar to that found for the cat areas (Mellott and others 2005). For PPF, the cytoarchitecture and corticocollicular projection also resemble those seen in cat A2 (compare our Fig. 10 with Fig. 7 in Winer and others 1998). On the other hand, the physiological properties, including their tonotopic organization, of neurons recorded in ferret PEG more closely match those of cat PAF, whereas the responses of neurons located in the AEG are more like those of cat A2 (Bizley and others 2005). Another possibility is that area VP in the ferret could be equivalent to field T in the cat. Further physiological exploration of these fields and examination of thalamocortical connectivity are clearly required in order to establish the correspondence between the auditory fields in ferret PEG and those in other species.

In the anterior bank, the homology between area AES in ferret and cat has already been pointed out (Ramsay and Meredith 2004; Manger and others 2005), although further work is needed to determine how far this region extends over the gyrus. Cortical injections in AEG (see Fig. 11) resulted in a labeling pattern in the midbrain quite similar to that produced by tracer injections into the cat insular cortex (see Winer and others 1998, Fig. 9). However, cytoarchitectonic features of the

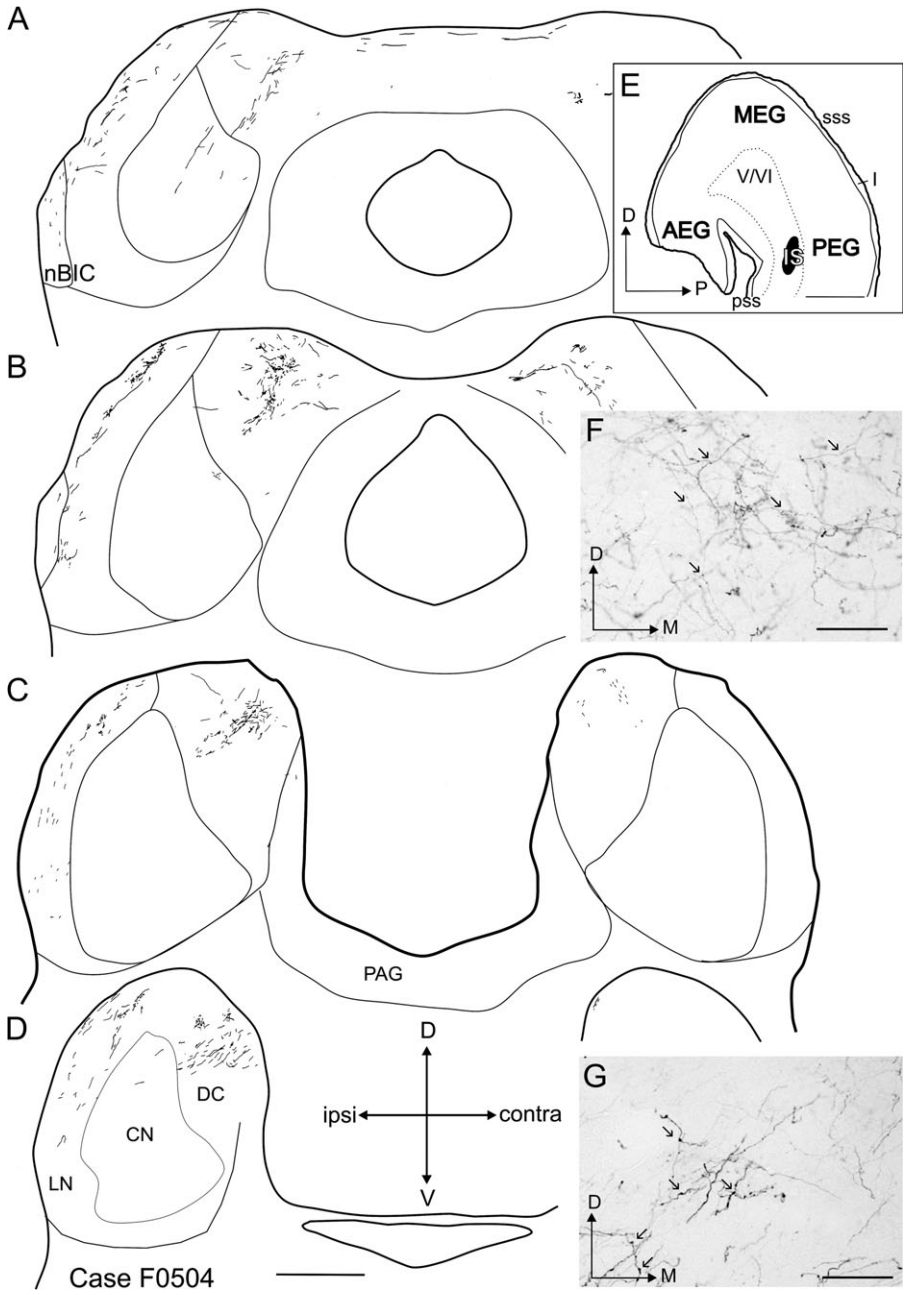

Figure 10. Anterograde labeling observed in the IC after a BDA injection in the PEG. Sections are ordered from rostral to caudal (*A–D*). The terminal fields are located in the ipsilateral LN and in the DC bilaterally. Some labeled fibers are observed in the nucleus of the brachium of the inferior colliculus (nBIC). The IS is shown in (*E*), and details of the terminal fields in the ipsilateral DC are shown in (*F*) and (*G*), with arrows pointing at labeled terminals. In general, these terminals are larger than those shown in Figures 7 and 8. Scale bar is 1 mm in (*A–D*), 2 mm in (*E*), and 50 μm in (*F*) and (*G*). I, Layer I of the cortex; contra, contralateral; D, dorsal; ipsi, ipsilateral; M, medial; P, posterior; V, ventral.

cat insular cortex (Clascá and others 1997) suggest that this cortical region in the ferret is likely to be located more rostrally on the AEG and not adjacent to the *pss* where the IS shown in Figure 11 was located. On the other hand, the pattern of corticocollicular labeling that we observed is similar to that described for cat temporal area of the auditory cortex (area Te) (Winer and others 1998), which in that species is located ventral and posterior to the insular area. One possibility therefore is that the area characterized physiologically as AVF might correspond to cat insular area and ADF to area Te, with area AES located mainly in the *pss*.

Descending Corticocollicular System in Mammals

The corticocollicular pathway has received much attention in the last few years and has now been described in several species (see Winer 2005, for review). The origins and targets of this pathway in the ferret (Fig. 12) are in broad agreement with the results of previous studies. For instance, as in other species, we found that the corticocollicular projection originates primarily from large pyramidal neurons in layer V and, to a much smaller extent, in layer VI. There are, however, certain differences that could be species specific and/or a limitation of the tracer techniques used, which have implications for the role of

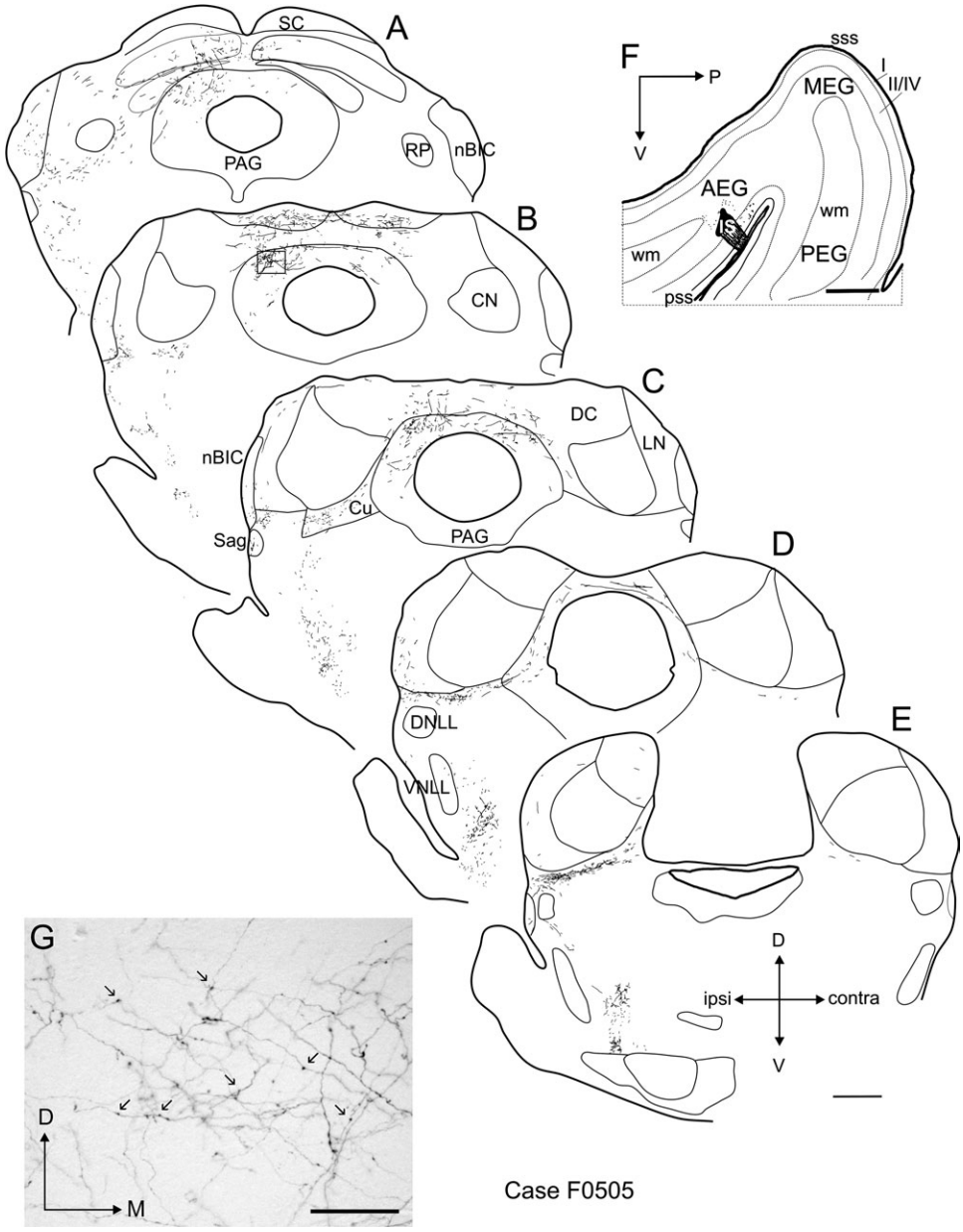

Figure 11. Anterograde labeling at the level of the IC observed after a BDA injection in the AEG. (*A–E*) drawings from rostral to caudal (300 μm apart) showing the terminal fields located bilaterally in the deeper layers of the SC and in the PAG. Ipsilaterally, terminal fields are found in the nucleus of the sagulum (Sag), nucleus of the brachium of the inferior colliculus (nBIC), LN, CN, ventral tegmental part of the IC, and surrounding paralemniscal regions and pontine nuclei. The IS is shown in (*F*) on a drawing of a flattened tangential section of the EG at the level of the center of this site. The main target is the PAG and examples of terminals found there are shown in (*G*). The terminal fields in PAG exhibit a low terminal density. Scale bar is 1 mm (*A–E*), 2 mm in (*F*), and 50 μm in (*G*). I, layer I of the cortex; II/IV, layers from II to IV of the cortex; contra, contralateral; Cu, cuneiform nucleus; D, dorsal; DNLL, dorsal nucleus of the lateral lemniscus; ipsi, ipsilateral; M, medial; P, posterior; V, ventral; VNLL, ventral nucleus of the lateral lemniscus; w.m., white matter.

Table 2
Mean (±standard deviation) area (μm^2) of cell bodies labeled after several large injections in the IC (case F0061)

	MEG (n = 50)	PEG (n = 50)	AEG (n = 50)
Area	298 ± 121.23	262.85 ± 88.45	462.08 ± 121.23

Note: ANOVA ($F_{147,2}$ = 30.412, $P \leq 0.001$).

descending cortical pathways in modulating the activity of midbrain neurons.

As in the cat (Winer and others 1998; Winer 2005), regional variations exist in the size and target locations of ferret corticocollicular projections. In both species, the LN and DC of the IC receive convergent input from more than one cortical field. These projections are also divergent, with tonotopic cortical areas targeting more than one IC subdivision. Variations exist, however, among different species in the strength and origin of descending projections to the CN, which is the principal source of tonotopically organized ascending information to the thalamus. This is important given that most studies examining the effects on the midbrain of focal electrical stimulation of the auditory cortex have recorded from neurons in the CN of the IC (e.g., Yan and Suga 1998; Ma and Suga 2001; Yan and Ehret 2002; Yan and others 2005). In the cat, the CN is

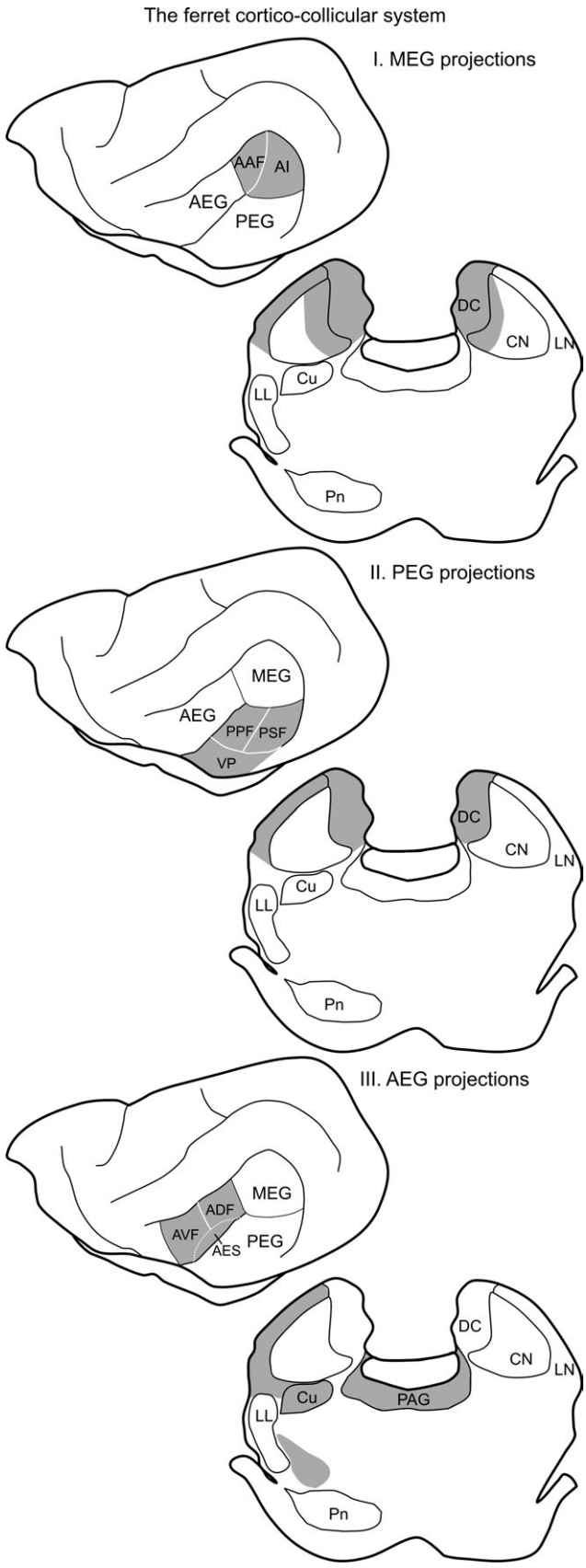

innervated by thin axons with few boutons, which originate from both primary and nonprimary cortical areas (Winer 2005), whereas in the ferret, the primary auditory fields in the MEG provide the only source of descending input to the CN. Moreover, the projection to the CN appears to be more robust in ferrets than in cats, suggesting that it may play a more important role in modulating auditory signal processing in these species. In the cat (Winer and Prieto 2001) and gerbil (Bajo and Moore 2005), distinct subpopulations of layer V projection neurons in core auditory cortex have been identified. We did not find this to be the case in the ferret, although this may be due to the fact that the dendritic trees of the pyramidal neurons were generally not completely filled.

The location of the corticocollicular terminals in the CN suggests a possible role in auditory processing and plasticity. We found that tracer injections in the MEG labeled terminal fields in the dorsal third of the CN, which have the same dorsomedial to ventrolateral orientation as the fibrodendritic laminae in this nucleus (Fig. 8). These laminae correspond to the isofrequency contours of the CN, which also extend into the DC (Casseday and others 2002). Small tracer injections into different frequency regions of the MEG resulted in distinct bands of terminal labeling in the CN of the IC (Fig. 9). This pattern of labeling therefore indicates that the projection from the cortex to the CN is tonotopically organized and suggests that corticocollicular neurons can influence the activity of groups of IC neurons that are all tuned to the same sound frequency.

More specifically, these findings raise the possibility that the corticocollicular projection may play a role in fine-tuning sound localization. The banded terminal fields occupy dorsal CN laminae where ascending axons arrive from the dorsal cochlear nucleus (Oliver 2005), which is responsible for processing spectral localization cues (Young and Davis 2002). We have shown that adult ferrets can relearn to localize accurately after having their spatial cues altered by reversible occlusion of one ear and that this process of adaptation at least in part involves plasticity in the neural processing of spectral localization cues (Kacelnik and others 2006). Elimination of corticocollicular neurons disrupts the ability of ferrets to adapt to a unilateral earplug (Bajo and others 2006), suggesting that descending signals from the cortex might modulate the transmission of spectral information from the brainstem.

Although studies of the effects of cortical stimulation have focused so far on the CN, the principal IC targets are extralemniscal subdivisions, namely the LN and DC. Indeed, the LN is the only region of the ferret IC to be innervated by all 3 major regions of EG. As is the cat (Winer and others 1998), the descending projections to the LN are purely ipsilateral, although a crossed projection has been described in the gerbil (Budinger and others 2000; Bajo and Moore 2005). The location and morphology of corticocollicular terminals in the ipsilateral LN are also similar in ferret and cat (present results; Winer 2005). The functional organization and role of the LN are poorly understood. However, the LN receives convergent auditory and

Figure 12. Summary of the origin and distribution of descending corticocollicular projections in the ferret. Projections originating in the primary cortical fields target the LN of the IC on the same side and the DC and dorsal part of the CN on both sides. Neurons in the secondary auditory cortical fields on the PEG have the same targets as those located in primary areas but exclude the CN. Neurons located in the AEG primarily innervate the tegmental midbrain. Cu, cuneiform nucleus; LL, lateral lemniscus; Pn, pontine nuclei.

tactile inputs (Aitkin and others 1981) and projects to the deeper layers of the SC (Edwards and others 1979; King and others 1998), where multisensory maps of space are found. Cortical modulation of the activity of LN neurons may therefore also be involved in spatial processing.

Conclusions

This study shows that descending corticocollicular projection neurons are found throughout the EG in the ferret and that the dorsomedial and lateral regions of the auditory midbrain receive distinct patterns of input. The recent increase in anatomical data on the organization of the corticocollicular pathway in different species contrasts with the paucity of functional studies. It seems certain that descending signals from the cortex will modulate the flow of ascending information during normal hearing and contribute to the neural computations that are carried out in the midbrain. A number of specific functions, mostly focused around associative learning (Suga and others 2002), have been proposed for the descending pathway from the auditory cortex to the IC. Behavioral as well as physiological studies are now required in order to elucidate these functions in the context of other descending loops and in the general context of auditory signal processing.

Notes

This work was supported by the Wellcome Trust, through a Senior Research Fellowship to AJK and by the Medical Research Council, UK. *Conflict of Interest*: None declared.

Address correspondence to Dr Victoria M. Bajo, Department of Physiology, Anatomy, and Genetics, Sherrington Building, Oxford University, Parks Road, Oxford OX1 3PT, UK. Email: Victoria.bajo@physiol.ox.ac.uk.

Funding to pay the Open Access publication charges for this article was provided by the Wellcome Trust.

References

Adams JC. 1981. Heavy metal intensification of DAB-based HRP reaction product. J Histochem Cytochem 29:775.

Aitkin LM, Kenyon CE, Philpott P. 1981. The representation of the auditory and somatosensory systems in the external nucleus of the cat inferior colliculus. J Comp Neurol 196:25–40.

Alitto HJ, Usrey WM. 2003. Corticothalamic feedback and sensory processing. Curr Opin Neurobiol 13:440–445.

Bajo VM, Moore DR. 2002. Convergence of ascending and descending auditory pathways in the ferret inferior colliculus. Central Auditory Processing: Integration of Auditory and Non-Auditory Information; 2002 May 12–15; Monte Veritá/Ascona, Switzerland. http://www.unifr.ch/neuro/rouiller/pdf/abstractbookfinal.pdf. (Accessed 20 March 2006).

Bajo VM, Moore DR. 2005. Descending projections from the auditory cortex to the inferior colliculus in the gerbil, *Meriones unguiculatus*. J Comp Neurol 486:101–116.

Bajo VM, Nodal FR, Moore DR, King AJ. 2006. Role of auditory cortex and descending corticocollicular projection in adaptation to altered binaural cues by adult ferrets. Abstr Assoc Res Otolaryngol 29:56.

Bizley JK, Nodal FR, Bajo VM, Moore DR, King AJ. 2003. Establishing cytoarchitectonics divisions in ferret auditory cortex. Abstr Assoc Res Otolaryngol 26:52.

Bizley JK, Bajo VM, Nodal FR, King AJ. 2006. Cortico-cortical connectivity of ferret auditory cortex. Abstr Assoc Res Otolaryngol 29:237–238.

Bizley JK, Nodal FR, Nelken I, King AJ. 2005. Functional organization of ferret auditory cortex. Cereb Cortex 15:1637–1653.

Budinger E, Heil P, Scheich H. 2000. Functional organization of auditory cortex in the mongolian gerbil (*Meriones unguiculatus*). IV. Connections with anatomically characterized subcortical structures. Eur J Neurosci 12:2452–2474.

Buonomano DV, Merzenich MM. 1998. Cortical plasticity: from synapses to maps. Annu Rev Neurosci 21:149–186.

Casseday JH, Fremouw T, Covey E. 2002. The inferior colliculus: a hub for the central auditory system. In: Oertel D, Fay RR, Popper AN, editors. Integrative functions in the mammalian auditory pathway. New York: Springer. p 238–318.

Clascá F, Llamas A, Reinoso-Suárez F. 1997. Insular cortex and neighboring fields in the cat: a redefinition based on cortical microarchitecture and connections with the thalamus. J Comp Neurol 384:456–482.

Depireux DA, Simon JZ, Klein DJ, Shamma SA. 2001. Spectro-temporal response field characterization with dynamic ripples in ferret primary auditory cortex. J Neurophysiol 85:1220–1234.

Edwards SB, Ginsburgh CL, Henkel CK, Stein BE. 1979. Sources of subcortical projections to the superior colliculus in the cat. J Comp Neurol 184:309–329.

Elhilali M, Fritz JB, Klein DJ, Simon JZ, Shamma SA. 2004. Dynamics of precise spike timing in primary auditory cortex. J Neurosci 24:1159–1172.

Fritz J, Elhilali M, Shamma SA. 2005. Differential dynamic plasticity of A1 receptive fields during multiple spectral tasks. J Neurosci 25:7623–7635.

Fritz J, Shamma S, Elhilali M, Klein D. 2003. Rapid task-related plasticity of spectrotemporal receptive fields in primary auditory cortex. Nat Neurosci 6:1216–1223.

Fuentes-Santamaria V, Alvarado AC, Brunso-Bechtold JK, Henkel CK. 2003. Upregulation of calretinin immunostaining in the ferret inferior colliculus after cochlear ablation. J Comp Neurol 460:585–596.

Henkel CK, Fuentes-Santamaria V, Alvarado JC, Brunso-Bechtold JK. 2003. Quantitative measurement of afferent layers in the ferret inferior colliculus: DNLL projections to sublayers. Hear Res 177:32–42.

Izzo PN, Graybiel AM, Bolam JP. 1987. Characterization of substance P- and [Met]enkephalin-immunoreactive neurons in the caudate nucleus of cat and ferret by a single section Golgi procedure. Neuroscience 20:577–587.

Jen PH-S, Chen QC, Sun XD. 1998. Corticofugal regulation of auditory sensitivity in the bat inferior colliculus. J Comp Physiol A 183:683–697.

Kacelnik O, Nodal FR, Parsons CH, King AJ. 2006. Training-induced plasticity of auditory localization in adult mammals. PLoS Biol 4:e71.

Kelly JB, Kavanagh GL, Dalton JC. 1986. Hearing in the ferret (*Mustela putorius*): thresholds for pure tone detection. Hear Res 24:269–275.

Kelly JB, Wong D. 1981. Laminar connections of the cat's auditory cortex. Brain Res 212:1–15.

King AJ, Jiang ZD, Moore DR. 1998. Auditory brainstem projections to the ferret superior colliculus: anatomical contribution to the neural coding of sound azimuth. J Comp Neurol 390:342–365.

King AJ, Parsons CH. 1999. Improved auditory spatial acuity in visually deprived ferrets. Eur J Neurosci 11:3945–3956.

Kowalski N, Versnel H, Shamma SA. 1995. Comparison of responses in the anterior and primary auditory fields of the ferret cortex. J Neurophysiol 73:1513–1523.

Lee CC, Winer JA. 2005. Principles governing auditory cortex connections. Cereb Cortex 15:1804–1814.

Ma X, Suga N. 2001. Corticofugal modulation of duration-tuned neurons in the midbrain auditory nucleus in bats. Proc Natl Acad Sci USA 98:14060–14065.

Manger PR, Engler G, Moll CK, Engel AK. 2005. The anterior ectosylvian visual area of the ferret: a homologue for an enigmatic visual cortical area of the cat? Eur J Neurosci 22:706–714.

Manger PR, Masiello I, Innocenti GM. 2002. Areal organization of the posterior parietal cortex of the ferret (*Mustela putorius*). Cereb Cortex 12:1280–1297.

Manger PR, Nakamura H, Valentiniene S, Innocenti GM. 2004. Visual areas in the temporal cortex of the ferret (*Mustela putorius*). Cereb cortex 14:676–689.

Marsh RA, Fuzessery ZM, Grose CD, Wenstrup JJ. 2002. Projection to the inferior colliculus from the basal nucleus of the amygdala. J Neurosci 22:10449–10460.

Mellot JG, Van der Gucht E, Lee CC, Larue DT, Winer JA, Lomber SG. 2005. Subdividing cat primary and non-primary auditory areas in the cerebrum with neurofilament proteins expressing SMI-32. Abstr Assoc Res Otolaryngol 28:348.
Merzenich MM, Brugge JF. 1973. Representation of the cochlear partition of the superior temporal plane of the macaque monkey. Brain Res 50:275–296.
Moore DR, Semple MN, Addison PD. 1983. Some acoustic properties of neurons in the ferret inferior colliculus. Brain Res 269:69–82.
Mrsic-Flogel TD, King AJ, Schnupp JWH. 2005. Encoding of virtual acoustic space stimuli by neurons in ferret primary auditory cortex. J Neurophysiol 93:3489–3503.
Mrsic-Flogel TD, Versnel H, King AJ. 2006. Development of contralateral and ipsilateral frequency representations in ferret primary auditory cortex. Eur J Neurosci 23:780–792.
Nelken I, Bizley JK, Nodal FR, Ahmed B, Schnupp JWH, King AJ. 2004. Large-scale organization of ferret auditory cortex revealed using continuous acquisition of intrinsic optical signals. J Neurophysiol 92:2574–2588.
Nodal FR, Bajo VM, Bizley JK, King AJ. 2006. Corticothalamic connectivity of ferret auditory cortex. Abstr Assoc Res Otolaryngol 29:238.
Oliver DL. 2005. Neuronal organization of the inferior colliculus. In: Winer JA, Schreiner CE, editors. The inferior colliculus. New York: Springer-Verlag. p 69–114.
Pallas SL, Sur M. 1993. Visual projections induced into the auditory pathway of ferrets: II. Corticocortical connections of primary auditory cortex. J Comp Neurol 337:317–333.
Phillips DP, Judge PW, Kelly JB. 1988. Primary auditory cortex in the ferret (*Mustela putorius*): neural response properties and topographic organization. Brain Res 443:281–294.
Ramsay AM, Meredith MA. 2004. Multiple sensory afferents to ferret pseudosylvian sulcal cortex. Neuroreport 15(3):461–465.
Redies H, Sieben U, Creutzfeldt OD. 1989. Functional subdivisions in the auditory cortex of the guinea pig. J Comp Neurol 282:473–488.
Saldaña E, Feliciano M, Mugnaini E. 1996. Distribution of descending projections from primary auditory neocortex to inferior colliculus mimics the topography of intracollicular projections. J Comp Neurol 371:15–40.
Stein BE. 2005. The development of a dialogue between cortex and midbrain to integrate multisensory information. Exp Brain Res 166:305–315.
Suga N, Xiao Z, Ma X, Ji W. 2002. Plasticity and corticofugal modulation for hearing in adult animals. Neuron 36:9–18.
Tsytsarev V, Yamazaki T, Ribot J, Tanaka S. 2004. Sound frequency representation in cat auditory cortex. Neuroimage 23:1246–1255.
Versnel H, Mossop JE, Mrsic-Flogel TD, Ahmed B, Moore DR. 2002. Optical imaging of intrinsic signals in ferret auditory cortex. J Neurophysiol 88:1545–1557.
Wallace MN, Roeda D, Harper MS. 1997. Deoxyglucose uptake in the ferret auditory cortex. Exp Brain Res 117:488–500.
Wallace MN, Rutkowski RG, Palmer AR. 2000. Identification and localisation of auditory areas in guinea pig cortex. Exp Brain Res 132:445–456.
Winer JA. 1992. The functional architecture of the medial geniculate body and the primary auditory cortex. In: Webster DB, Popper AN, Fay RR, editors. Springer handbook of auditory research. Volume 1. The mammalian auditory pathway: neuroanatomy. New York: Springer-Verlag. p 222–409.
Winer JA. 2005. Three systems of descending projections to the inferior colliculus. In: Winer JA, Schreiner CE, editors. The inferior colliculus. New York: Springer-Verlag. p 231–247.
Winer JA, Larue DT, Diehl JJ, Hefti BJ. 1998. Auditory cortical projections to the cat inferior colliculus. J Comp Neurol 400: 147–174.
Winer JA, Miller LM, Lee CC, Schreiner CE. 2005. Auditory thalamocortical transformation: structure and functions. Trends Neurosci 28:255–263.
Winer JA, Prieto JJ. 2001. Layer V in cat primary auditory cortex (AI): cellular architecture and identification of projection neurons. J Comp Neurol 434:379–412.
Wong D, Kelly JB. 1981. Differentially projecting cells in individual layers of the auditory cortex: a double-labeling study. Brain Res 230: 362–366.
Yan J, Ehret G. 2002. Corticofugal modulation of midbrain sound processing in the house mouse. Eur J Neurosci 16:119–28.
Yan W, Suga N. 1998. Corticofugal modulation of the midbrain frequency map in the bat auditory system. Nat Neurosci 1:54–58.
Yan J, Zhang Y, Ehret G. 2005. Corticofugal shaping of frequency tuning curves in the central nucleus of the inferior colliculus of mice. J Neurophysiol 93:71–83.
Young EI, Davis KA. 2002. Circuitry and function of the dorsal cochlear nucleus. In: Oertel D, Fay RR, Popper AN, editors. Integrative functions in the mammalian auditory pathway. New York: Springer. p 160–206.
Zhou X, Jen PH-S. 2000. Brief and short-term corticofugal modulation of subcortical auditory responses in the big brown bat, *Eptesicus fuscus*. J Neurophysiol 84:3083–3087.